Escuela Superior Politécnica del Litoral

Facultad de Ingeniería en Electricidad y Computación

Investigation of the Impact of Adopting Different Regulation Curves in the Accommodation of PV Generators to Distribution Systems

Integrator Project

Prior to Obtaining the Degree:

Electrical Engineer

Presented by:
Diana Isabel Montenegro Curillo
Franklin Jefferson Saquinga Sangoquiza

Guayaquil - Ecuador
Year: 2023

Dedication

I dedicate my project to my family, who have been a cornerstone throughout my entire formation as an engineer, and to Franklin Saquinga, my partner, who has provided me with unwavering support and encouragement through all the ups and downs of the project and my life.

Diana Montenegro

Dedication

This investigative work is dedicated to my sister Angy, my grandmother Rosario, my partner Diana Montenegro and my family who became a source of motivation throughout my career and they taught me that no matter the difficulties that arise in life, you can always find a ray of light even in the darkest night.

Franklin Saquinga

Acknowledgements

My entire gratitude goes to God; without Him, none of this could have been accomplished. I am also grateful for having had the opportunity to meet professors who trusted and believed in my abilities and who shared their knowledge to help me reach this point, namely M.Sc. Jimmy Córdova and Ph.D. Miguel Torres. Finally, my sincerest thanks to Post-Doc. Fernanda Trindade and M. Eng. Iván Endara for their guidance and time in the development and completion of this project, which I am confident will serve as a guide for future research endeavors, whether in this same field or another.

Diana Montenegro

Acknowledgements

My sincere gratitude to professors Miguel Torres, Fernanda Trindade, and Iván Endara for their assistance, and above all, for their valuable time dedicated to addressing each of the doubts that arose during this research.

Franklin Saquinga

Declaración Expresa

“Los derechos de titularidad y explotación, nos corresponde conforme al reglamento de propiedad intelectual de la institución; Diana Isabel Montenegro Curillo y Franklin Jefferson Saquinga Sangoquiza y damos nuestro consentimiento para que la ESPOL realice la comunicación pública de la obra por cualquier medio con el fin de promover la consulta, difusión y uso público de la producción intelectual"

Diana Montenegro

Franklin Saquinga

Evaluators

Ivan Endara Firmado digitalmente por Ivan Endara Fecha: 2024.02.16 20:30:00 -05'00'

Iván Endara

Subject teacher

Firmado electrónicamente por: OTTO ISMAEL ALVARADO MORENO

Otto Alvarado

Project tutor

Abstract

Over the past few years, distributed generation with solar sources has been integrated into the distribution network. The power system control equipment installed prior to the large accommodation of photovoltaic (PV) generators is not designed to protect the system against overvoltages occurring at point of common coupling. Therefore, it is essential to appropriately set the control modes through regulation curve adjustments included in smart inverters to help mitigate voltage stability issues in the network from the perspectives of generation and distribution, that are areas where PV systems are most commonly installed. Besides, it is crucial to assess the effectiveness of the selected Volt-Watt and Volt-var curves through the simulation of the IEEE 34 bus medium voltage distribution system, with the incorporating PV generators using the software OpenDSS and Python. The results of the simulation demonstrated that the Volt-var curves had better performance in the implemented system as they prevented voltage violations, and the output power of the affected photovoltaic systems remained close to the maximum capacity.

Key words: Distributed generation, overvoltage, Volt-var curve, Volt-Watt curve.

General index

Abbreviations

ANSI	American National Standards Institute
DER	Distributed energy resources
EPS	Electric Power System
IEEE	Institute of Electrical and Electronics Engineers
PCC	Point of common coupling
Pmpp	Power at the maximum power point
PVS	Photovoltaic Systems
VV	Volt-var
VW	Volt-Watt

Symbology

V	Volt
kV	Kilovolt
W	Watt
kW	Kilowatt
var	Volt amper reactive
kvar	Kilovolt amper reactive
va	Volt amper
kva	Kilovolt amper
pu	Per unit
T	Temperature
pf	Power factor

Index of figures

Table index

Chapter 1

1.1 Introduction

In recent years, electricity consumption per capita has been shown to be higher than the growth of the world population [1], so the most energetically and economically feasible solution is to implement distributed energy resources (DER). Currently, distributed energy from photovoltaic (PV) generators is one of the most used; just in 2022 the total worldwide capacity of them was 1’053,12 GW [2], 13.3% more than it was 10 years ago. Due to this accelerated increase, the electrical system has begun to have some challenges in terms of energy quality and service, because the control equipment that was usually placed along the lines is being affected by the injection of additional active power to the grid [3].

The area of the electrical power system where there is the greatest load density and the effect of the high integration of distributed energy is in the distribution system. The nature of the load often has a great influence on operational and planning decisions [4], and this is more seen when there is greater density of it, so PV generators installed in large part of them will make the service delivered by the distribution utility not to have the same quality as without DERs. The most recurring problems due to adoption of PV generators are related to stable state voltage, voltage imbalances, line losses, overload in transformers, and others [5]. As far as the consumption units are concerned, they are affected according to [6] in their production of solar energy, electricity bill, and need to oversize the equipment; depending on where the inverter is connected in the feeder.

The solutions that have been proposed for the adoption of PV generators are many, but in which it will focus and assess its impact on this research are in the regulatory curves provided by smart investors (SI). The control curves selected will be the Volt-Watt and Volt-VAR, which allow active and reactive power control, to prevent violations of parameters such as voltage, in the distribution network, from the points of view of generation and distribution.

1.2 Problem description

The use of distributed energy resource (DER) in its initial years had a low penetration to the network and a large geographical dispersion; therefore, it did not affect the voltage of the network and the large distribution companies or users who used this resource, so they maintained the use of voltage control through equipment such as On-load tap changer (OLTC), voltage regulators (VRs) and shunt capacitors (SC) [7]. However, the penetration of DER from photovoltaic sources over time has been increasing, and they are usually used for residential, industrial, commercial, street lighting, and other loads. As a result, the massive insertion of photovoltaic generators involves a large number of problems at the distribution level which directly affect the quality of electrical energy [8, 9]; of which harmonic distortions, steady-state voltage problems, voltage regulation; could be highlighted.

1.3 Justification

From the perspective of the photovoltaic (PV) generator owner, the energy benefit may be reduced if the distributed generator helps in regulating the voltage of the electrical network. This happens because the PV generator may have its active power supply reduced or require the inverter to be oversized. Therefore, studies and methodologies are also necessary to obtain a compromise solution for the regulation curves that benefit simultaneously the two points of view: generation and distribution.

1.4 Objectives

1.4.1 General objective

Analyze the impact of the adoption of different regulation curves on the accommodation of photovoltaic generators to distribution systems, using an IEEE test feeder, to evaluate the effect on the voltage from the point of view of generation and distribution.

1.4.2 Specific objectives

1. Select a case study from the IEEE for the installation of a large accommodation of distributed photovoltaic generation.
2. Establish the continuous operation limits of the feeder for proper voltage operation according to ANSI C84.1 - 2020 and IEEE 1547™ - 2018 standards.
3. Implement the mode of power regulation curves in terms of voltage in smart inverters according to the ranges specified by the IEEE 1547™ - 2018 standard.
4. Compare the impact of Volt-Watt and Volt-var curve from both perspectives to identify the curve control that enhances energy quality and power production in the selected system.

1.5 Theoretical framework

In this section, the main concepts that will be addressed in the research will be shown, such as: distributed generation, smart inverters, photovoltaic generators, two types of regulation curves that will be used: Volt-Watt and Volt-VAR; accommodation capacity, and others.

1.5.1 Distributed generation

The distributed generation (DG) can be known with different expressions such as decentralized generation, dispersed or embedded generation [10]. Currently, there is not universal definition of DG because it may be based either on one of the ratings of the plant or on the voltage level to which the embedded generation is connected [11]. For this reason, based on our thesis topic and in accordance with of The International Energy Agency, where they define it as “a source of electric energy that is linked directly to the distribution network to provide a neighborhood energy-user and corroborates de distribution network” [11, p. 1].

On the other hand, there are some common attributes of DG such as not centrally planned (by the utility), nor centrally dispatched, normally smaller than 50-100 MW and usually connected to the distribution system [11].

1.5.2 Distributed energy resources

Distributed Energy Resources (DER) refer to small-scale energy resources that are directly connected to low voltage (LV) and medium voltage (MV) networks of the electric power system (EPS), ensuring that there is no dependence or not required (extreme cases) of bulk power transmission systems. It should be noted that DER units can be made up of generation units such as fuel cells, photovoltaics systems, micro-turbines, batteries, flywheels, superconducting magnetic energy storage, and others. Below is a figure showing the technologies that DERs may have [12, 13].

Figure 1.1

Distributed energy resources technologies **[12]**

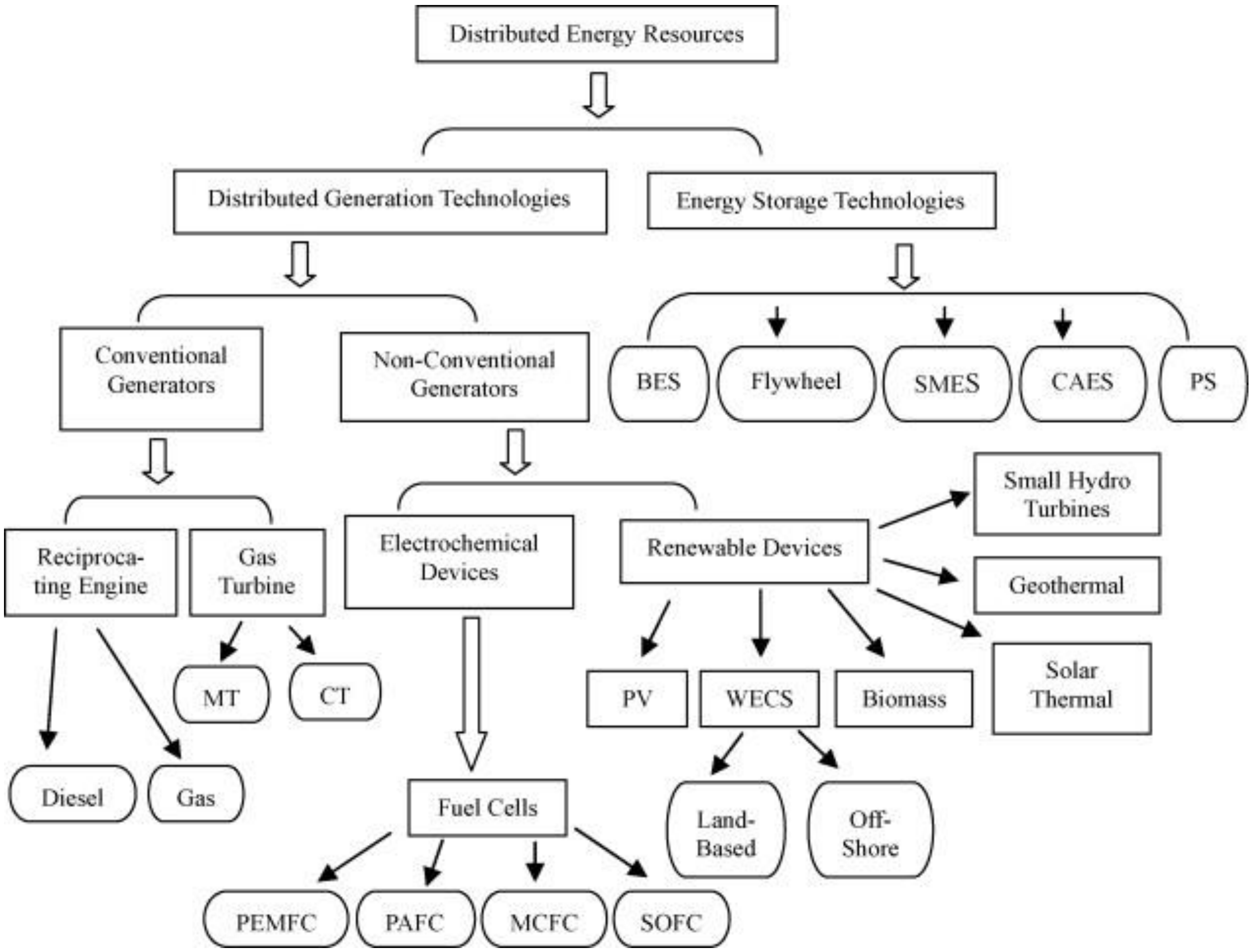

Note. Figure from Distributed Energy Resources and Benefits to the Environment (2010).

1.5.3 PV generators

Photovoltaic generators are composed of an array of modules connected in parallel and series, with characteristics according to the type of load and inverter to which it is connected, such as: open voltage (V_{oc}), short circuit current (I_{sc}) and point maximum power (Pmmp). In fact, PV generators are basically modeled as a source of nonlinear current of limited power, by its internal structure, which also has functions of constant current and voltage depending on the point at which it is operated [14].

1.5.4 Smart inverters

To define an intelligent inverter, it is necessary to know what "Smart" means within the context of the device, which is the ability to do something efficiently and automatically without the operator being there all the time. On the other hand, the "inverter" that was initially in charge of converting from DC to AC or vice versa, has had some advances due to the increase in distributed generation. In recent years, inverter technology has developed and has come to have control functions such as power flow, sense faults, automatic disconnection, and others. Therefore, smart inverters are the thought and processing components of micro networks [15], and as they are included in the DER, they must comply with IEEE 1457™ - 2018 standard. Moreover, the main indicators of smart inverters are shown in the following Figure:

Figure 1.2

Smart inverter indicators **[15]**

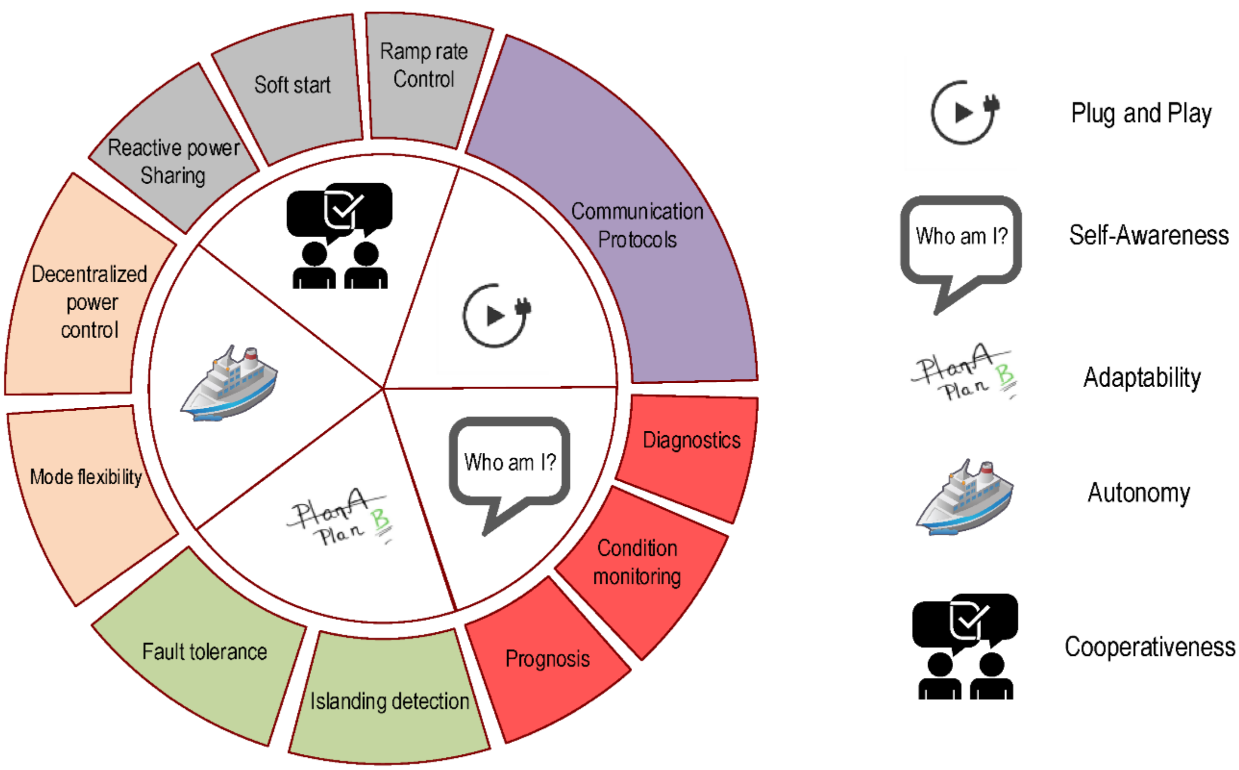

Note. Figure from Smart Inverters for Microgrid Applications: A Review (2019).

Each indicator shall be described below.

- Plug and Play: Inverters that have this feature can contact all communication protocols that are handled in the micro network [15].
- Self- Awareness: This feature allows smart inverters to monitor the status of the device, also diagnose to identify the source of failures and thus make a forecast to identify if a failure will occur [15].
- Adaptability: it is an important characteristic because the inverter must adapt to changes that occur in the network, and this is done by estimating parameters (network impedances) and self-synchronizations in terms of frequency [15].
- Autonomy: due to the different configurations that are made in the microgrid, smart inverters, to act autonomously, use the drooping method to control the power flow, so that inverters do not use communication protocols when they are at great distances [15].
- Cooperativeness: smart inverters must work together with other network elements, to get a balance in the system parameters [15].

1.5.5 Volt-Watt curve

Volt-Watt (VW) curves is a mode of the smart inverter in which the active power output is monitored and adjusted as a function of the voltage at the point of common coupling (PCC) [16], following a linear behavior as shown in the figure:

Figure 1.3

Volt-Watt curve characteristic [13]

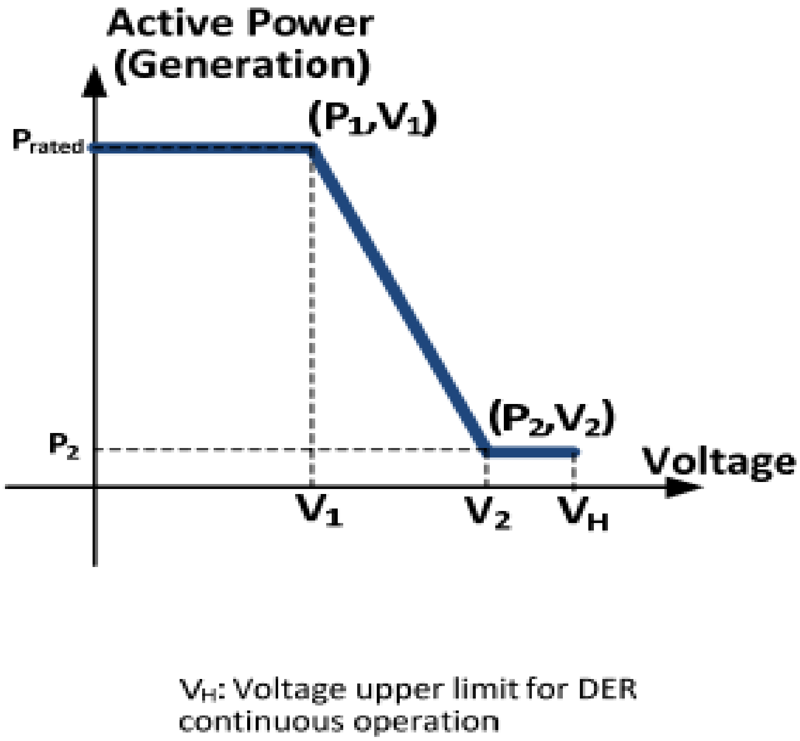

Note. Figure from IEEE Standard for Interconnection and Interoperability of Distributed Energy Resources with Associated Electric Power Systems Interfaces (2018).

The active power and voltage values can be set through the values established by the Electrical Power Systems (EPS) Operator of the area or through the Standard for Interconnection and Interoperability of Distributed Energy Resources with Associated Electric Power Systems Interface (IEEE 1547^{TM}-2018) [13].

1.5.6 Volt-var curve

Volt-var (VV) curves correspond to a mode of smart inverters, by means of which reactive power is controlled according to the terminal voltage of the inverter. When the voltage drops from a specific level, the VV control injects reagents, while, if the voltage rises, reagents are absorbed [17]. The following figure illustrates the above.

Figure 1.4

Volt-var curve characteristic [13]

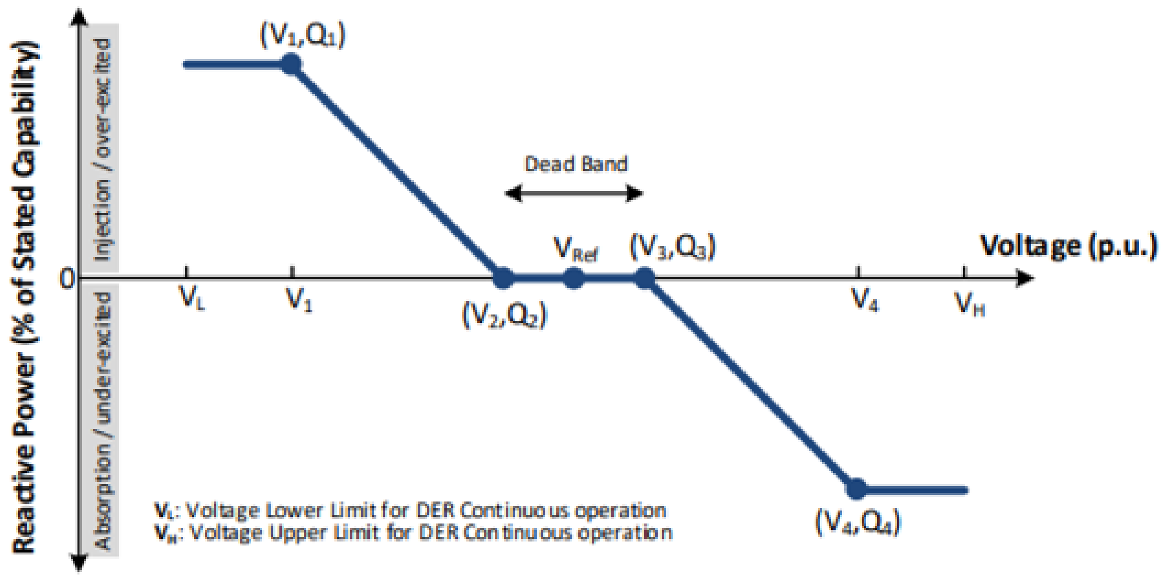

Note. Figure from IEEE Standard for Interconnection and Interoperability of Distributed Energy Resources with Associated Electric Power Systems Interfaces (2018).

The reactive power and voltages values can be set by the utility EPS of the area or set by Standard IEEE 1547™-2018.

1.5.7 Accommodation capacity

It is determined by quantifying the DERs that can be included in the distribution system without affecting the technical limits established by the standards, without affecting the quality and reliability of the energy service. The restrictive factors of the accommodation capacity are those that are related to the characteristics of the renewable energy, load characteristic, load growth rate, line capacity and system peak shaving capacity.

Furthermore, this term allows us to quantify the available power capacity and the effectiveness of the regulation curves, so if the accommodation increases the regulation curves are efficient.

1.5.8 Voltage and reactive power regulation

Based on the IEEE 1547^{TM}-2018 standard, the following voltage and reactive power values are defined for the proper operation of a DER connected to a distribution grid, but first the types of categories will be defined.

Category A: they are the minimum capacities necessary for voltage regulation of the EPS and they are reasonably achievable by all DER technologies that have a lower penetration in distribution systems. Furthermore, energy production is not subject to frequent large variations [13].

Category B: It meets all the requirements of category A, but this includes the missing capabilities to integrate DER technologies in EPS that have greater penetration and frequent large variations [13].

Figure 1.5

Minimum reactive power injection and absorption capability [13]

Category	Injection capability as % of nameplate apparent power (kVA) rating	Absorption capability as % of nameplate apparent power (kVa) rating
A (at DER rated voltage)	44	25
B (over the full extent of ANSI C84.1 range A)	44	44

Note. Figure from IEEE Standard for Interconnection and Interoperability of Distributed Energy Resources with Associated Electric Power Systems Interfaces (2018).

In general, the DER must be capable of injecting or absorbing active power for levels greater than or equal to the minimum active power capacity in steady state or 5% of the rated power (Prated), but in case it is greater than 5% and less than 20%, the parameters in Figure 5 must be used multiplied by the active power output and divided by 20% of the nominal active power

[13]. Another case that can be found is when the active power output is greater than 20%, in this case the parameters in Figure 1.15 must be used as required by the installed control function [13].

Voltage regulation is done through active power and reactive power as shown in the following Figures.

Figure 1.6

Setting of voltage - active power for Category A and B of DER [13]

Voltage-active power parameters	Default settings	Ranges of allowable settings	
		Minimum	Maximum
V_1	1.06 V_N	1.05 V_N	1.09 V_N
P_1	P_{rated}	N/A	N/A
V_2	1.1 V_N	V_1 + 0.01 V_N	1.10 V_N
P_2 *(applicable to DER that can only generate active power)*	The lesser of 0.2 P_{rated} or P_{min}[a]	P_{min}	P_{rated}
P'_2 *(applicable to DER that can generate and absorb active power)*	0[b]	0	P'_{rated}
Open Loop Response Time	10 s[c]	0.5 s	60 s

Note. Figure from IEEE Standard for Interconnection and Interoperability of Distributed Energy Resources with Associated Electric Power Systems Interfaces (2018).

Figure 1.6 shows the parameters in which the voltage is set so that the DER can inject or absorb active power to mitigate system overvoltage. It should be noted that this follows a linear characteristic, and its parameters can be configured locally or remotely through the EPS operator [13].

Figure 1.7

Setting of voltage - reactive power for Category A and B of DER [13]

Voltage-reactive power parameters	**Default settings**		**Ranges of allowable settings**	
	Category A	**Category B**	**Minimum**	**Maximum**
V_{Ref}	V_N	V_N	0.95 V_N	1.05 V_N
V_2	V_N	$V_{Ref} - 0.02\ V_N$	Category A: V_{Ref} Category B: $V_{Ref} - 0.03\ V_N$	V_{Ref} [c]
Q_2	0	0	100% of nameplate reactive power capability, absorption	100% of nameplate reactive power capability, injection
V_3	V_N	$V_{Ref} + 0.02\ V_N$	V_{Ref} [c]	Category A: V_{Ref} Category B: $V_{Ref} +$ 0.03 V_N
Q_3	0	0	100% of nameplate reactive power capability, absorption	100% of nameplae reactive power capability, injection
V_1	0.9 V_N	$V_{Ref} - 0.08\ V_N$	$V_{Ref} - 0.18\ V_N$	$V_2 - 0.02\ V_N$ [c]
Q_1 [a]	25% of nameplate apparent power rating, injection	44% of nameplate apparent power rating, injection	0	100% of nameplate reactive power capability, injection [b]
V_4	1.1 V_N	$V_{Ref} + 0.08\ V_N$	V_3+0.02 V_N [c]	$V_{Ref} + 0.18\ V_N$
Q_4	25% of nameplate apparent power rating, absorption	44% of nameplate apparent power rating, absorption	100% of nameplate reactive power capability, absorption	0
Open loop response time	10 s	5 s	1 s	90 s

Note. Figure from IEEE Standard for Interconnection and Interoperability of Distributed Energy Resources with Associated Electric Power Systems Interfaces (2018).

Figure 1.7 indicates the adjustment parameters carried out by the DER to control the output reactive power in terms of voltage. An important detail is that these parameters can be configured locally or remotely depending on the EPS operator [13].

Chapter 2

2.1 Methodology

This section will describe the methodology used for this investigative work, where the impact of the regulation curves using the IEEE 34 bus distribution feeder was determined through simulations in quasi-static time series (QSTS) mode, and with a photovoltaic generation in a period of 24 hours in steps of 15 minutes, through the open source programs OpenDSS and Python. The regulation curves chosen were Volt-Watt and Volt-var because in recent years, the accommodating capacity of photovoltaic generators in distribution systems has increased. This has led overvoltage and power quality issues at certain spots in the network. Therefore, it is necessary to investigate the impact of each control curve to mitigate voltage problems in steady state during the significant integration of distributed energy from photovoltaic systems.

2.1.1 IEEE 34 bus test feeder modeling

The IEEE 34 bus system is a feeder located in Arizona that operates at 24.9 kV but in one of its sections has a transformer that reduces the voltage to 4.16 kV [18].This system has different types of loads such as unbalanced, concentrated and distributed, which are mostly connected in the middle of the lines as shown in Figure 2.1. Also, it is a network that has two voltage regulators, overhead and underground lines, capacitors on the lines that act as a voltage compensator at nodes 844 and 848.

Figure 2.1

IEEE 34-bar feeder schematic diagram

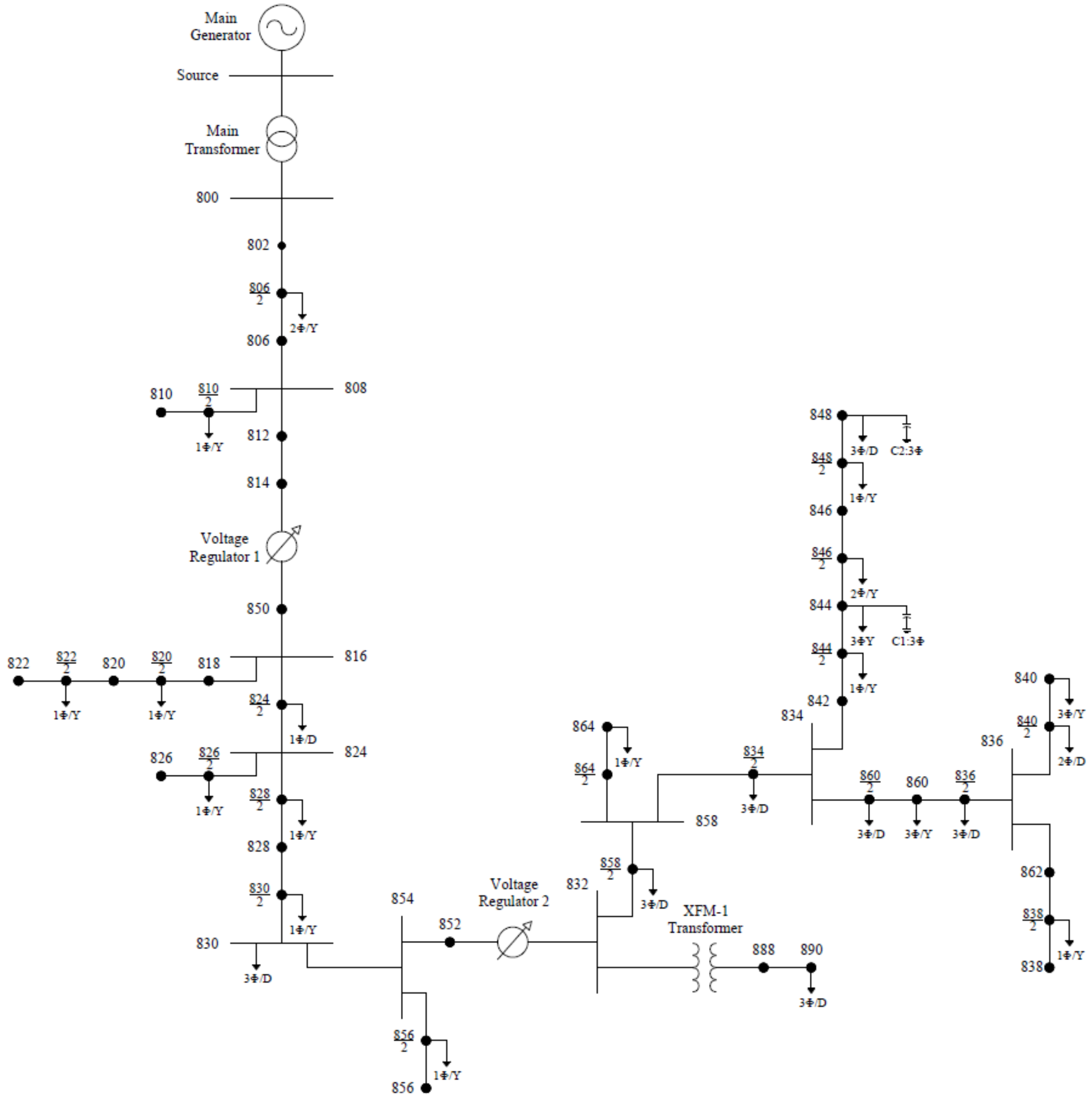

Note. Own elaboration.

The parameters of diverse network elements, including lines, loads, voltage regulators, and others, are comprehensively detail in OpenDSS software code, where the network is modeled. **¡Error! No se encuentra el origen de la referencia.** and **¡Error! No se encuentra el origen de la referencia.** provide a comprehensive overview of the specifications associated with the transformers and compensators used in the feeder. Note: The information for the remaining elements is found in Appendix A.

Table 2.1

Transformer data

Transformer	Capacity (kVA)	kV-High	kV-Low	R %	X %
Main Transformer	2500	69 - D	24.9 Gr. Y	1	8
XFM -1	500	24.9 – Gr.W	4.16 – Gr.W	1.9	4.08

Note. Data taken from Distribution System Analysis Subcommittee - IEEE 34 Node Test Feeder (2017).

Table 2.2

Capacitor data

Node	Phase A (kVAr)	Phase B (kVAr)	Phase C (kVAr)
844	100	100	100
848	150	150	150

Note. Data taken from Distribution System Analysis Subcommittee - IEEE 34 Node Test Feeder (2017).

2.1.2 Photovoltaic insertion modeling

The modeling of photovoltaic systems (PVS) was executed using Python software due to its capability to manipulate the output power of PV systems over time, facilitating the analysis of the repercussions of increased distributed generation on the voltage at various nodes of the feeder. The configuration of each PV unit was implemented in accordance with the guidelines outlined in the OpenDSS program manuals. Figure 2.2 shows the many variables that can be included in the model of a real PVS.

It’s worth to mention that OpenDSS was not the sole tool utilized throughout the research. The reason for this is that managing a substantial number of modifications and comparisons within this program becomes inherently intricate. Conversely, in Python, the process of altering and comparing data from other software under various photovoltaic integration scenarios proves to be more practical.

Figure 2.2

Block Diagram of the Photovoltaic System Element Model in OpenDSS

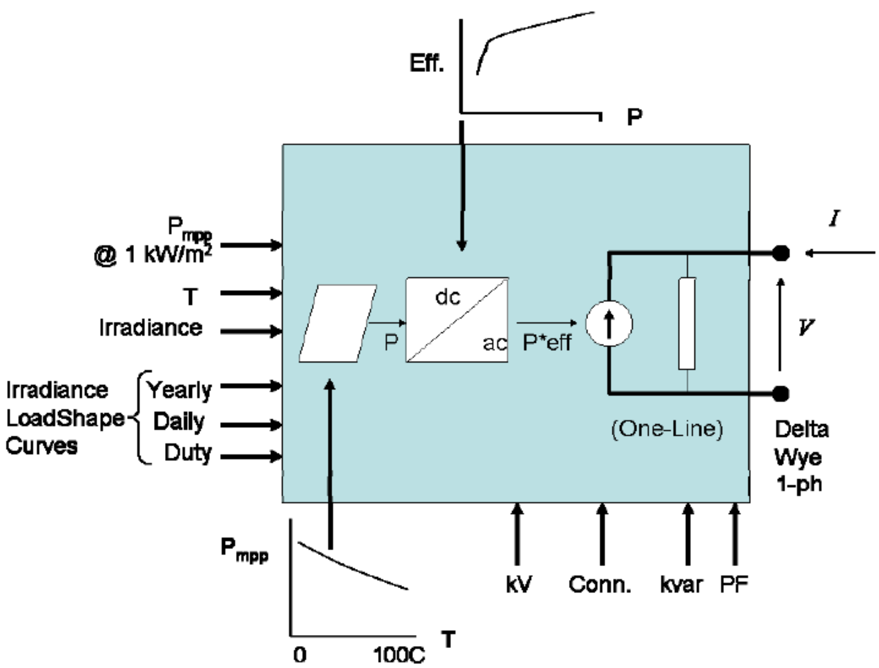

Note. Figure from OpenDSS PV System Element Model (2011).

Figure 2.2 exhibits the variables included into the model, emphasizing that the PV unit and the inverter are represented as a single element. The most known variables for modeling are: Pmpp (Power at the maximum power point), T (temperature), Irradiance (the instantaneous radiation incident on a surface), kV (voltage level of the PV system), Conn. (connection type, default: wye), kvar (reactive power), PF (power factor), and others. Where, kvar and PF can be highlighted because those are the variables that allow the inverter to inject or absorb reactive power from the connected network. It is also essential to note the utilization of Irradiance LoadShape Curves, which facilitates the simulation of state changes over various time periods such as Yearly, Daily, or *Duty*. In this investigation, the *Daily* mode was employed to observe the function's behavior over a period of 24 hours [19].

Based on the preceding parameters, each PV system could be setting in Python, **¡Error! No se encuentra el origen de la referencia.** details the features incorporated in the setups. The nodes at which the PV units were located were: 840, 844, 848, 860, 816, 830, and 858, as illustrated in Figure 2.3. Besides, the seven distributed systems operate simultaneously, so if one generates 0, 500, or 1000 kW, all will do so as the case may be.

Table 2.3

Features of PV units

Variable	Value	Unit
Phases	3	-
Bus1	840	-
kV	24.9	kV
kva	1000	kva
P_{mpp}	0, 500 y 1000	kW
Temperature	25	ºC
PF	1	-
Daily	Irradiancia	pu

Note. Parameters set in Python to be executed in OpenDSS for each of the PV units.

Figure 2.3

Schematic diagram of IEEE 34 bus feeder with PVS

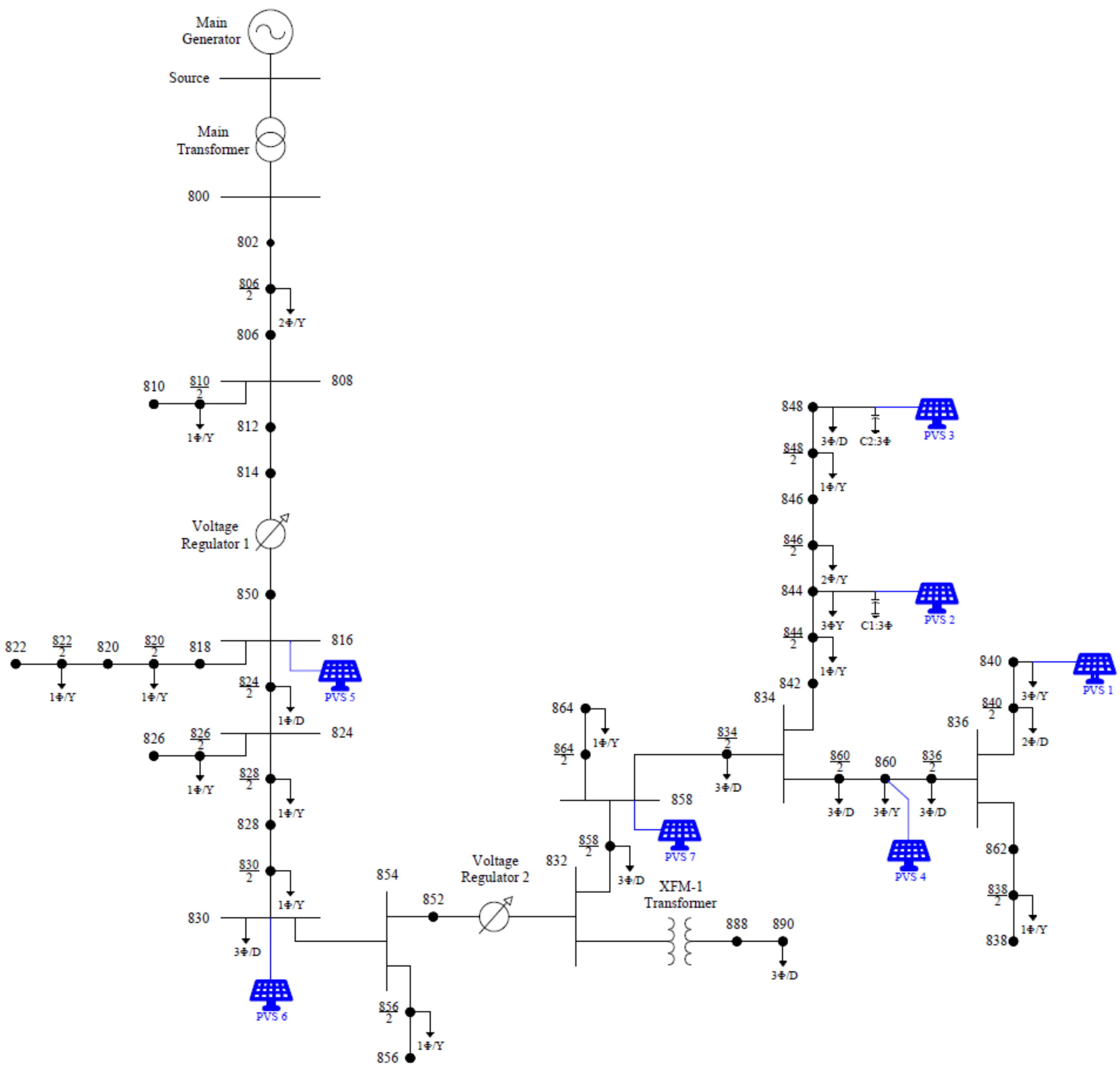

Note. Own elaboration.

The variables in **¡Error! No se encuentra el origen de la referencia.** such as kva, P_{mpp} and Daily are important to understand the behavior of the photovoltaic systems in the simulations. Below is information about them:

- kva: Maximum apparent power of the inverter.
- P_{mpp}: Maximum nominal power of the photovoltaic system for an irradiance of 1 kW/m^2 and a temperature of 25 ºC.
- Daily: Command used for state changes in a period of time, but a LoadShape object must be previously defined.

The LoadShape curve plays a significant role in system modeling as it is a multiplicative factor for the Irradiance data. Irradiance represents the sun's radiation power per unit area, measured in kW/m^2. In Python, the irradiation curve for each PV system was programmed with 96 points, covering a 24-hour period in steps of 15 minutes, as can be seen in Figure 2.4.

Figure 2.4

Irradiance factor curve

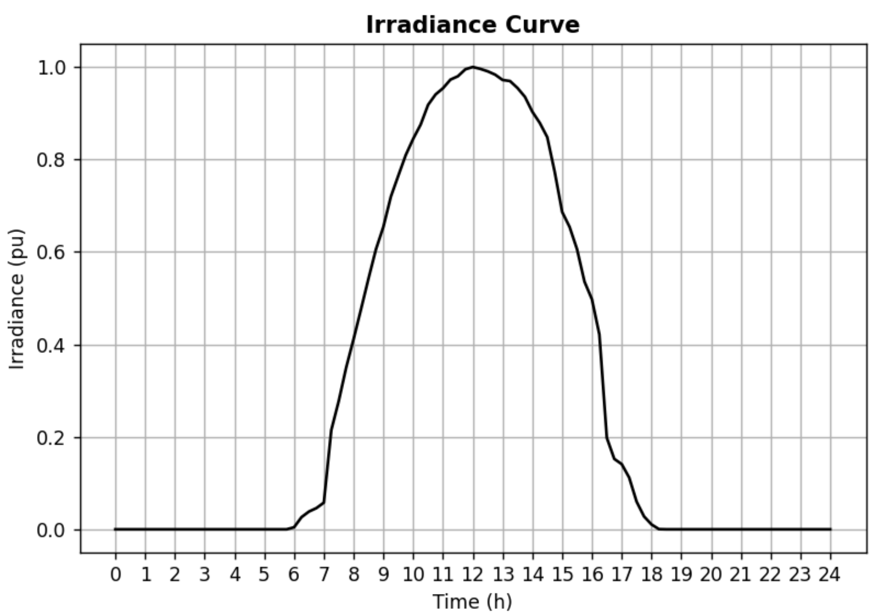

Note. Own elaboration.

The variable Pmpp was configured according to Regulation Number ARCERNNR 008/23 "Regulatory framework of distributed generation for the self-sufficiency of regulated consumers of electrical energy", which states that if there is electric power injection to a distribution network, the nominal power of the Distributed Generation System for Self-Supply (DGSS) must be limited to 2000 kW. The main reasons for this nominal power are to promote the adoption of clean technologies and alternative energies, and also to minimize the risk of electricity shortages during dry periods [20, 21].

The output power of photovoltaic systems is defined based on the following equation:

$$\boldsymbol{P_{PVS} = \left(P_{mpp}\right) \cdot (IF) \cdot (TF)} \tag{2.1}$$

Where,

P_{PVS}: Output power of a PV system in kW.

IF: Irradiance factor in per unit.

TF: Temperature factor. It is 1 because the chosen temperature is 25 ºC. (Figure 2.5 shows the graph of TF vs Temperature in per unit).

Figure 2.5

Temperature Factor vs. Temperature

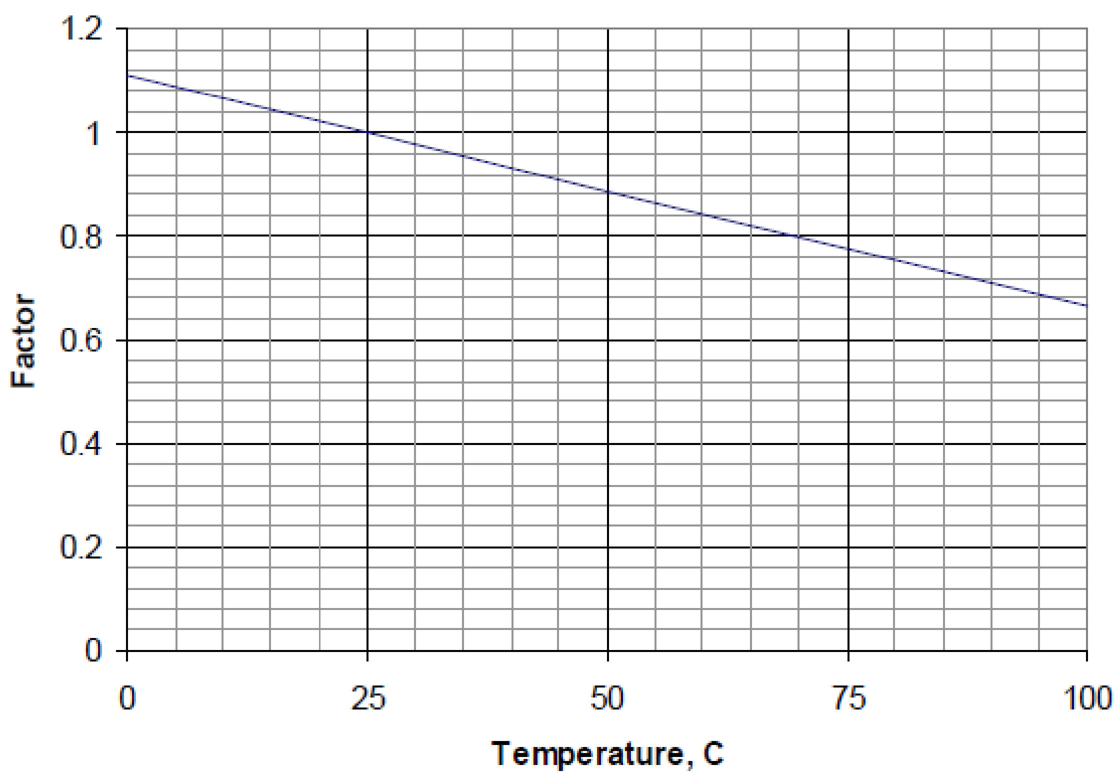

Note. Figure from OpenDSS PV System Element Model (2011).

2.1.3 Regulation Curves

The regulation curves employed in this investigation to mitigate overvoltage are Volt-Watt and Volt-var, based on the IEEE 1547™ - 2018 "IEEE Standard for Interconnection and Interoperability of Distributed Energy Resources with Associated Electric Power Systems Interfaces" and ANSI C84.1 - 2020 "Electric Power Systems and Equipment - Voltage Ratings (60 Hz)" standards [13, 22].

2.1.4 Modeling of Volt-Watt curve from the generation point of view

The IEEE 1547™ - 2018 standard was utilized to define the operational voltage limits for generation point of view, which ranged from 0.88 to 1.10 per unit. This facilitated the identification and setting of the appropriate curve points in OpenDSS and Python, detailed in **¡Error! No se encuentra el origen de la referencia.** [13].

Table 2.4

Settings of the Volt-Watt curve from the generation point of view

Variable	Voltage (pu)	Active Power (pu)
P_0	0.80	1
P_1	**1.08**	**1**
P_2	**1.10**	**0**
P_n	1.20	0

Note. Parameters set for the Volt-Watt curve in Python to be executed from OpenDSS.

From **¡Error! No se encuentra el origen de la referencia.**, points P_1 and P_2 played a crucial role in configuring the curve. Placing P_1 at 1.08 pu ensured that all voltages below this value have an active power output of 1 pu. On the other hand, P_2 is set at 1.10 pu with zero active power, preventing voltages above this threshold from experiencing overvoltage. Points P_0 and Pn give a reference configuration for the curve, and it is recommended that they be located at a significant distance from P_1 and P_2 to avoid adversely affecting the proper operation of the regulation curve. The following figure illustrates these points.

Figure 2.6

Volt-Watt curve and its setting points from the generation point of view

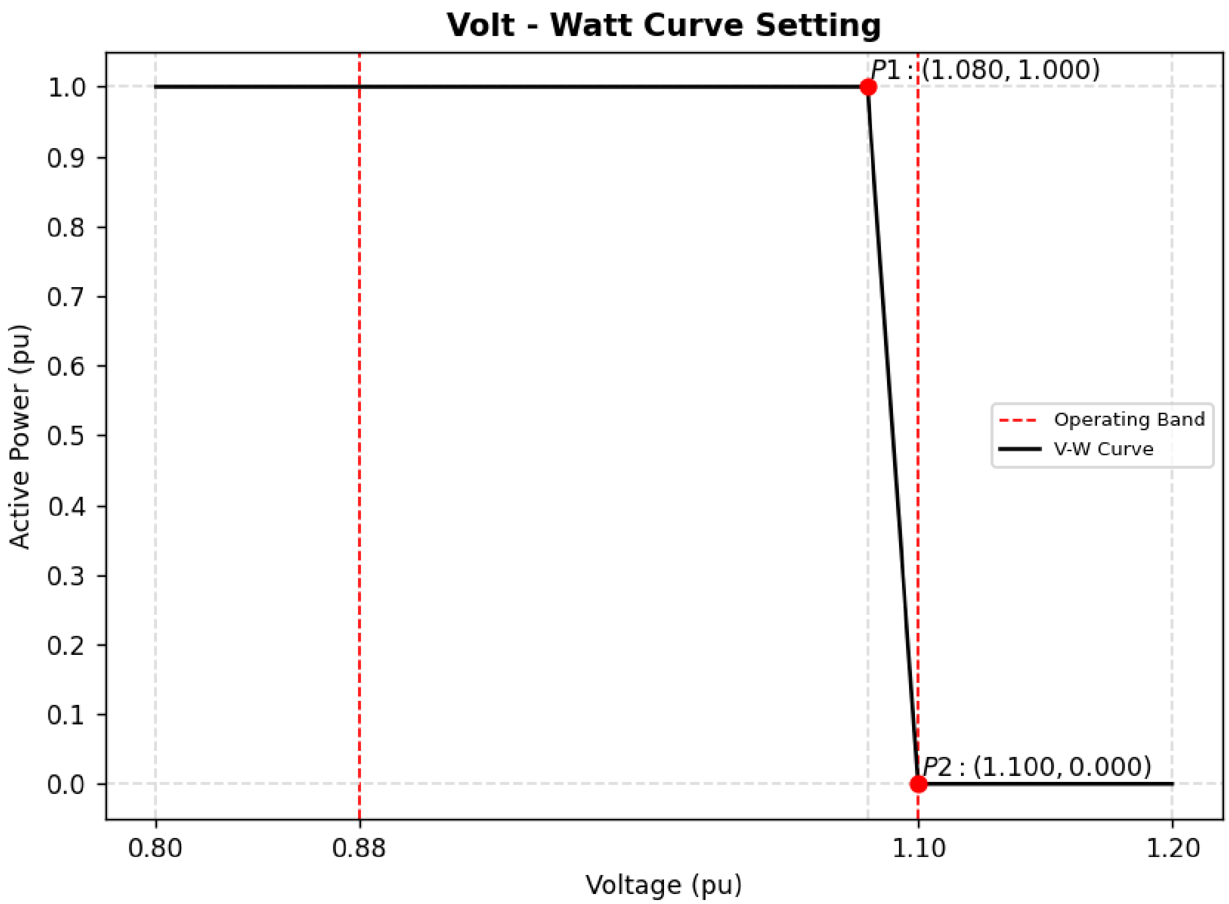

Note. Own elaboration.

In Figure 2.6, it was observed that the curve maintains the output power for all photovoltaic systems at their maximum capacity until reaching a voltage of 1.08 pu. Subsequently, the power decreases until reaching zero at a voltage of 1.10 pu. From point P_2 onwards, the output power of the PVS remains at zero to prevent the voltage from violating the limit specified in IEEE 1547™ - 2018 standard [13].

2.1.5 Modeling of Volt-var curve from the generation point of view

In the Volt-var curve, the standard from the previous section was also used as a reference to establish operational limits for voltage between 0.88 and 1.10 per unit. Likewise, this facilitated the determination of the six most suitable parameters for configuring the curve in OpenDSS and Python, as depicted in **¡Error! No se encuentra el origen de la referencia.** [13].

Table 2.5

Settings of the Volt-var curve from the generation point of view

Variable	Voltage (pu)	Reactive Power (pu)
P_0	0.80	0.44
P_1	**0.95**	**0.44**
P_2	**0.97**	**0**
P_3	**1.08**	**0**
P_4	**1.10**	**- 0.44**
P_n	1.25	- 0.44

Note. Parameters set for the Volt-var curve in Python to be executed from OpenDSS.

From Table 2.5, P_1, P_2, P_3, and P_4 were selected based on the parameter range specified in the IEEE 1547™ - 2018 standard. The aim was to make certain that the chosen points provide maximum hosting capacity, thereby mitigating issues in steady-state voltage. Besides, Po and P_n were selected for the same reason, as observed in the Volt-Watt curve.

Figure 2.7

Volt-var curve and its setting points from the generation point of view

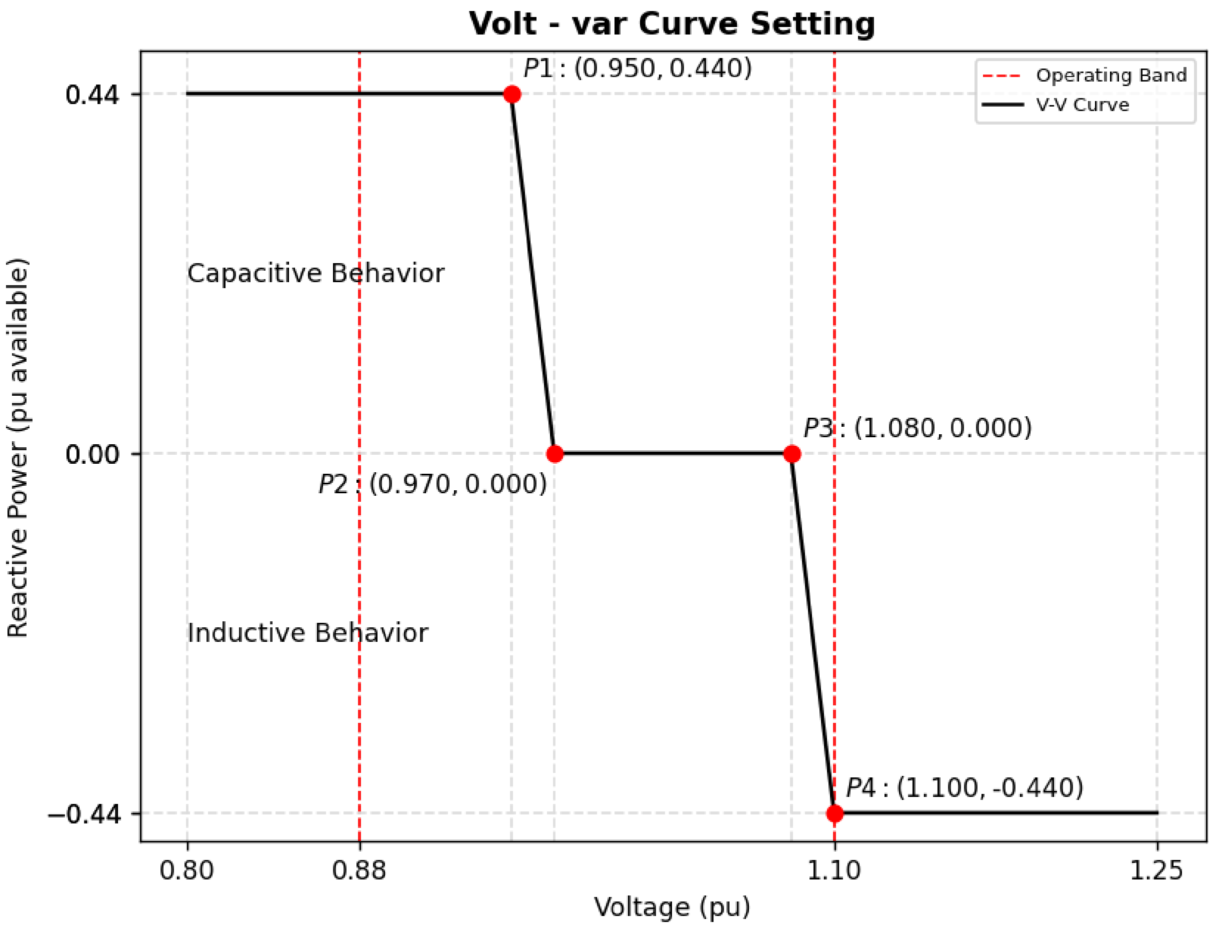

Note. Own elaboration.

In Figure 2.7, the Volt-var curve was plotted, displaying three operational regions. Examining it along the horizontal axis, voltage, it can be observed that from 0.80 to 0.97 per unit, there is a capacitive behavior, as the control elevates the voltage by injecting reactive power from the grid (positive reactive power). From 0.97 to 1.08 per unit, there is a segment where neither reactive power is absorbed nor injected, known as the dead-band. And from 1.08 to 1.25 per unit, there is an inductive behavior, meaning the voltage decreases as if a bank of reactors were placed in parallel.

For this research, only inductive behavior was considered, which had a maximum capacity to absorb reactive power from the grid to the inverter of 44% of the apparent power, equivalent to 440 kvar (Power Factor = 0.90 lagging and leading). The reactive power required by the smart inverter to mitigate overvoltage depends on Equation 2.2.

$$\boldsymbol{Q_A = \sqrt{(S_{SI})^2 - (P_{PVS})^2}} \quad (2.2)$$

Where,

Q_A: Reactive power absorbed from the grid by the smart inverter in kvar.

S_{SI}: Nominal apparent power of the inverter in kVA.

P_{PVS}: Output power of a photovoltaic system in kW.

2.1.6 Modeling of Volt-Watt curve from the distribution point of view

From the distribution perspective, Standards IEEE 1547™ - 2018 and ANSI C84.1 – 2020 were used to establish operational limits for voltage between 0.95 and 1.05 per unit and to configure the curves in the OpenDSS and Python software [22]. **¡Error! No se encuentra el origen de la referencia.** provides a detailed overview of the curve settings:

Table 2.6

Settings of the Volt-Watt curve from the distribution point of view

Variable	Voltage (pu)	Active Power (pu)
P_0	0.80	1
P_1	**1.02**	**1**
P_2	**1.10**	**0**
P_n	1.20	0

Note. Parameters set for the Volt-Watt curve in Python to be executed from OpenDSS.

Analogously to the generation perspective, P_1 and P_2 were selected. P_1 was defined at 1.02 pu based on the minimum average voltage of the nodes where the PV systems are located, while P_2 was set at 1.10 pu to harness the maximum amount of photovoltaic production. It is relevant to note that it wasn't configured at 1.05 pu, as one might intuitively think, due to a significant reduction in photovoltaic output power and inefficient control. In addition, points P_0 and P_n were a reference for plotting the curve, with values chosen to be distant from P_1 and P_2, avoiding any disruption to the proper operation of the method. The graph depicting the configured parameters can be observed in Figures 2.8.

Figure 2.8

Volt-Watt curve and its setting points from the distribution point of view

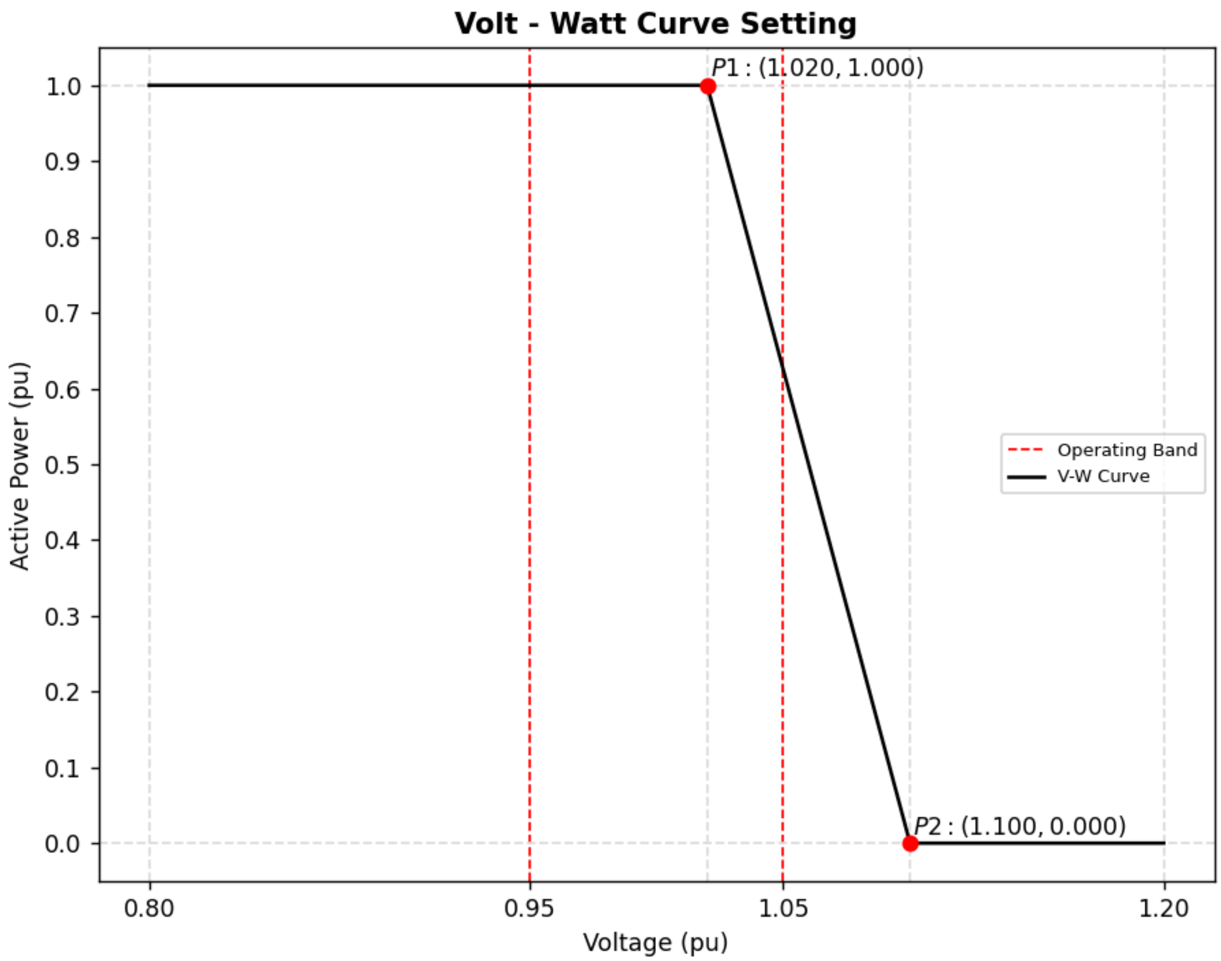

Note. Own elaboration.

With the configuration set in Figure 2.8, the seven photovoltaic units give their maximum power (1 pu = 1000 kW) until their voltage exceeds the value of 1.02 pu. From P_1 up to 1.10 pu, the power gradually decreases until reaching zero, preventing overvoltage at the PCC.

2.1.7 Modeling of Volt-var curve from the distribution point of view

The IEEE 1547™ - 2018 and ANSI C84.1 – 2020 standards were used as a reference, similar to the Volt-Watt curves from the same perspective. The voltage operating range was maintained between 0.95 and 1.05 pu, and the configurations of the curve variables were established as follows:

Table 2.7

Settings of the Volt-var curve from the distribution point of view

Variable	Voltage (pu)	Reactive Power (pu)
P_0	0.80	0.44
P_1	**0.95**	**0.44**
P_2	**0.98**	**0**
P_3	**1.02**	**0**
P_4	**1.05**	**- 0.44**
P_n	1.20	- 0.44

Note. Parameters set for the Volt-var curve in Python to be executed from OpenDSS.

Due to the fact that the curve in Figure 2.7. employs the same control method, albeit with different configuration settings, the explanation for this curve is the same, as is its modeling formula.

Figure 2.9

Volt-var curve and its setting points from the distribution point of view

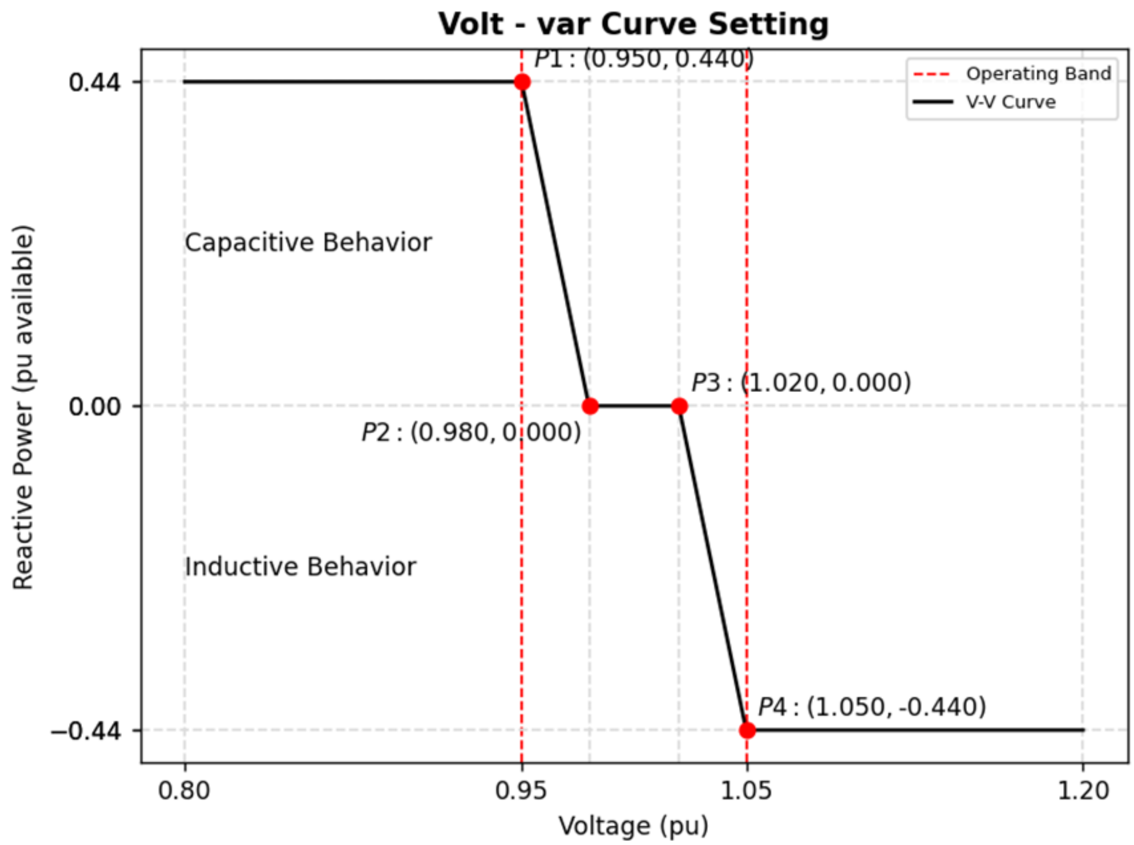

Note. Own elaboration.

It is crucial to note that the inductive behavior region of Figure 2.9 extends from 1.02 to 1.20 because of the minimum average voltage without applying regulation curves and the upper limit of the continuous operating band, respectively.

Chapter 3

3.1 Results

This section will present the simulation results in the absence of regulation curves when there is a large accommodation of photovoltaic generators in the selected feeder, following the parameters set by Standard IEEE 1547™ - 2018. The chapter will be divided into three sections. The first and second sections will show the results from the perspectives of generation and distribution, respectively. And, the third section will provide an analysis of the presented results.

3.2 Results from the generation point of view without voltage control

As mentioned in the previous chapter the limits of continuous operation for generation are 0.88 to 1.10 pu, in Figure 3.1 the state of the voltages is displayed at the nodes where the PV systems are connected without any regulation curve.

Figure 3.1

Voltages at the nodes of the PV units from the generation point of view. a) Voltage of PVS 1, 2, 3 and 4 b) Voltage of PVS 5 c) Voltage of PVS 6 d) Voltage of PVS 7

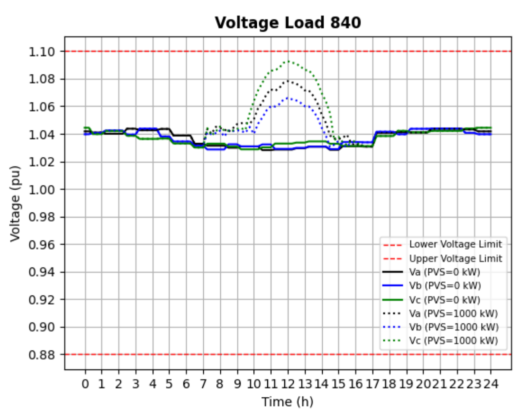

a)

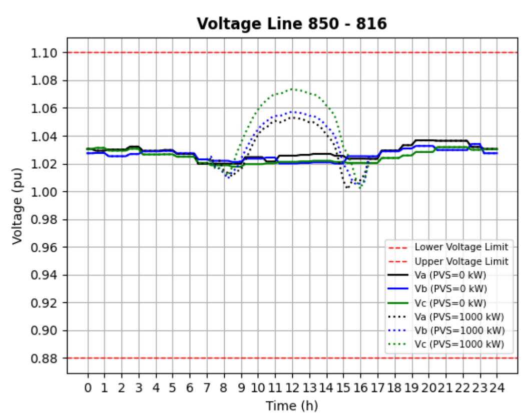

b)

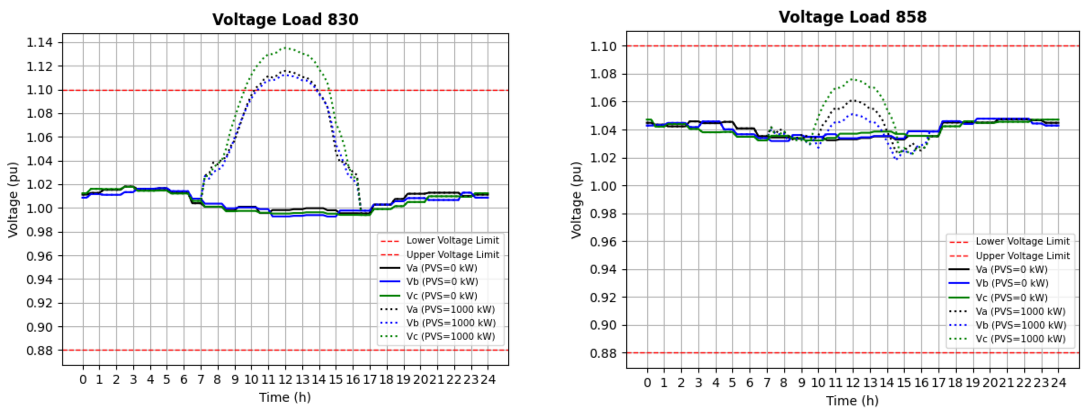

c) *d)*

Note. Own elaboration.

The voltage of node 840 corresponding to PVS 1 has a similar behavior to the photovoltaic systems 2, 3 and 4, as well as their maximum values, that's why in graph a) of Figure 3.1, one of them was shown. The following table summarizes all the voltage values at the time of highest irradiance (12 p.m.), the nodes in which they are connected and the proof of the assertion of similar voltages that was carried out:

Table 3.1

Maximum voltages before applying regulation curve

Node	PV system	PVS = 0 kW	PVS = 1000 kW
840	1	1.0440	1.0790
844	2	1.0443	1.0773
848	3	1.0447	1.0795
860	4	1.0442	1.0776
816	5	1.0342	1.0613
830	**6**	**0.9954**	**1.1210**
858	7	1.0450	1.0718

Note. Own elaboration.

The node where the greatest impact of the photovoltaic generator accommodation was observed was at node 830, as its average voltage rose to 1.1210 pu, exceeding the upper limit of the continuous operating band. Therefore, the results of the following subsections will focus on PVS 6.

3.2.1 Volt-Watt curve from the generation point of view

Upon activating the Volt-Watt curves mode, there was an observed a mitigation in the overvoltage at the studied node, and a significant reduction in the power production of its 1000 kW capacity. The following bar graphs show what was said:

Figure 3.2

Voltage applying Volt-Watt curve from the generation point of view

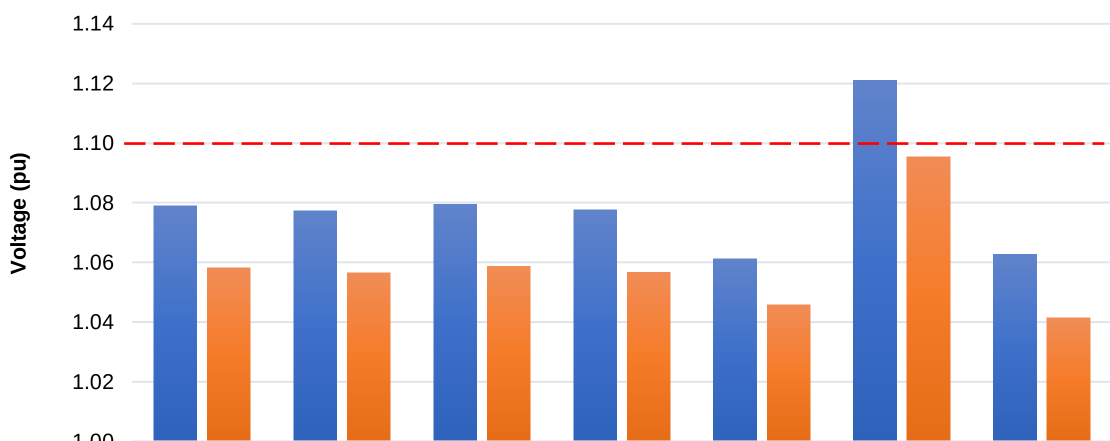

	840 (PVS 1)	844 (PVS 2)	848 (PVS 3)	860 (PVS 4)	816 (PVS 5)	830 (PVS 6)	858 (PVS 7)
Without Curve	1.0790	1.0773	1.0795	1.0776	1.0613	1.1210	1.0628
Volt-Watt Curve	1.0582	1.0565	1.0587	1.0567	1.0458	1.0954	1.0415

Note. Own elaboration.

Figure 3.3

Active Power applying Volt-Watt curve from the generation point of view

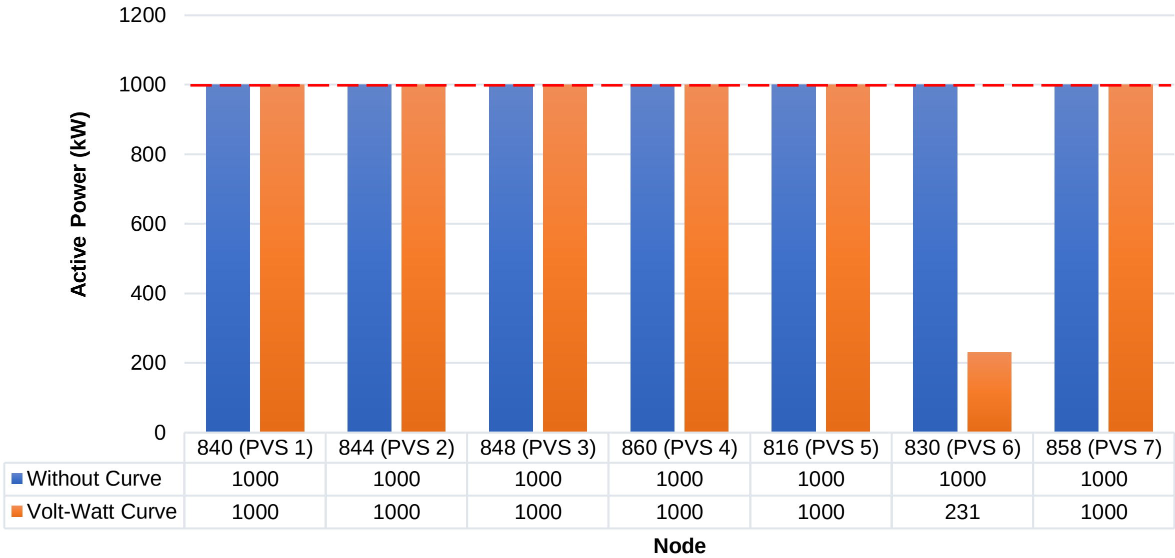

Note. Own elaboration.

The overvoltage at node 830 decreased to 1.09 pu, a value within the permissible operating range. However, this resulted in a reduction in active power at this location to 231 kW. To rectify this behavior and prevent significant losses in the generation system, the power output of PVS 6 was adjusted to 200 kW. In Figure 3.4 and Figure 3.5, the voltage and power results are displayed with the implemented change.

Figure 3.4

Voltage applying Volt-Watt curve when PV Generator 6 has an output of 200 kW

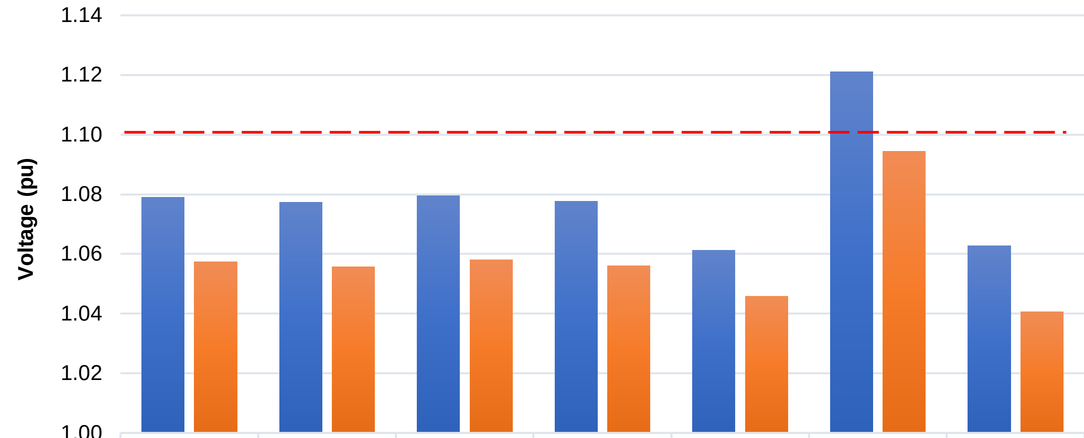

	840 (PVS 1)	844 (PVS 2)	848 (PVS 3)	860 (PVS 4)	816 (PVS 5)	830 (PVS 6)	858 (PVS 7)
Without Curve	1.0790	1.0773	1.0795	1.0776	1.0613	1.1210	1.0628
Volt-Watt Curve	1.0574	1.0557	1.0580	1.0560	1.0458	1.0944	1.0407

Node

Note. Own elaboration.

Figure 3.5

Power applying Volt-Watt curve when PV Generator 6 has an output of 200 kW

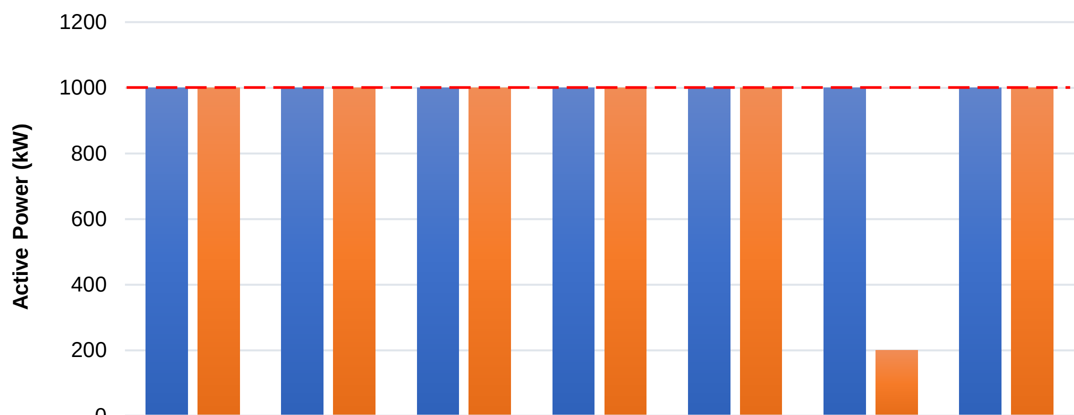

	840 (PVS 1)	844 (PVS 2)	848 (PVS 3)	860 (PVS 4)	816 (PVS 5)	830 (PVS 6)	858 (PVS 7)
Without Curve	1000	1000	1000	1000	1000	1000	1000
Volt-Watt Curve	1000	1000	1000	1000	1000	200	1000

Node

Note. Own elaboration.

With the change made a better result was obtained for the use of the curves Volt - Watt because the power output in all the photovoltaic systems are the maximum, despite the fact that one of the generators had to be asked to reduce its original power.

To demonstrate that the configuration of the Volt-Watt curves was appropriate, Figure 3.6 and Figure 3.7 were plotted, illustrating the curve settings at maximum voltage produced at noon, along with the corresponding power output.

Figure 3.6

Graph of the Volt-Watt curve with voltage and output power of the PVS 2

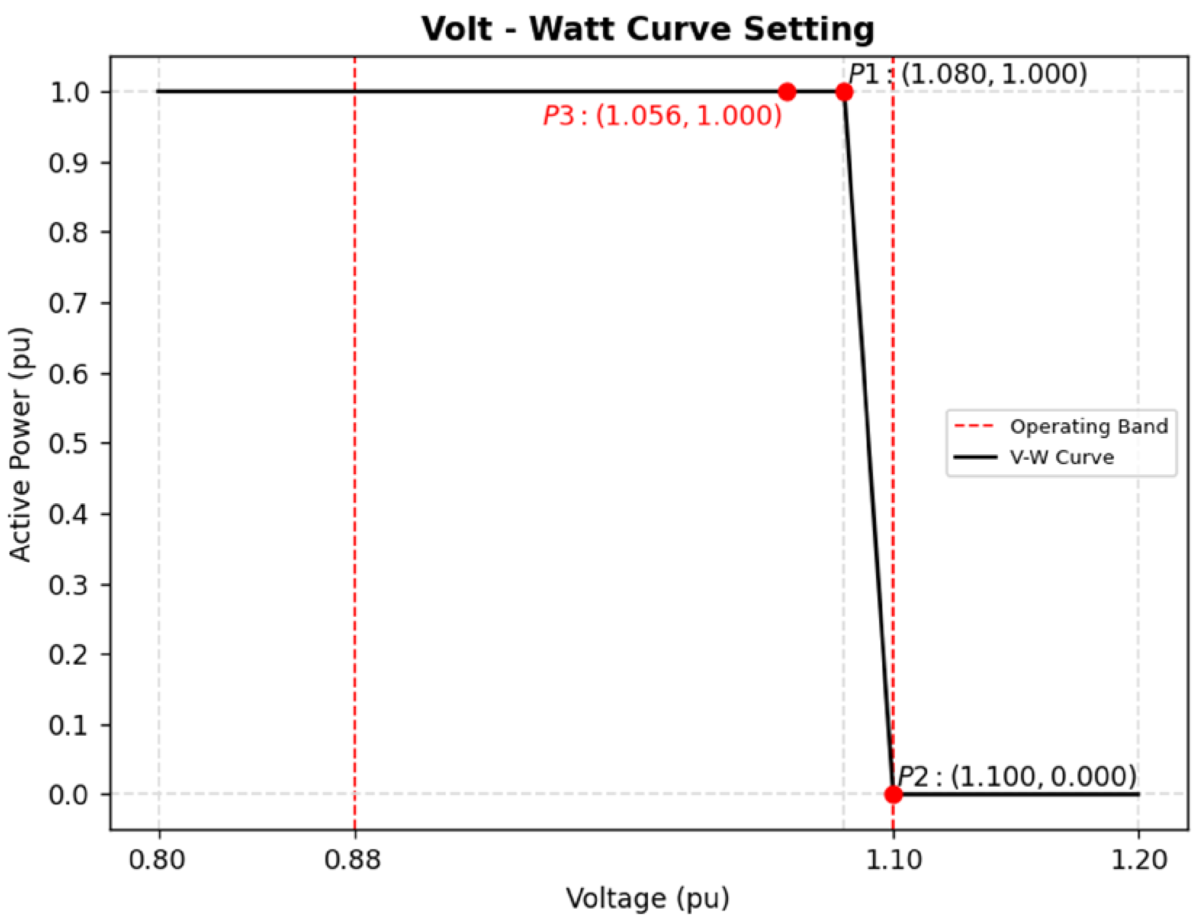

Note. Own elaboration.

Figure 3.6 specifically shows the variables of PVS 2, which is an example of a generator without overvoltage, and since its voltage is below 1.08 pu, the power output was at 1 pu (equivalent to 1000 kW).

Figure 3.7

Graph of the Volt-Watt curve with voltage and output power of the PVS 6

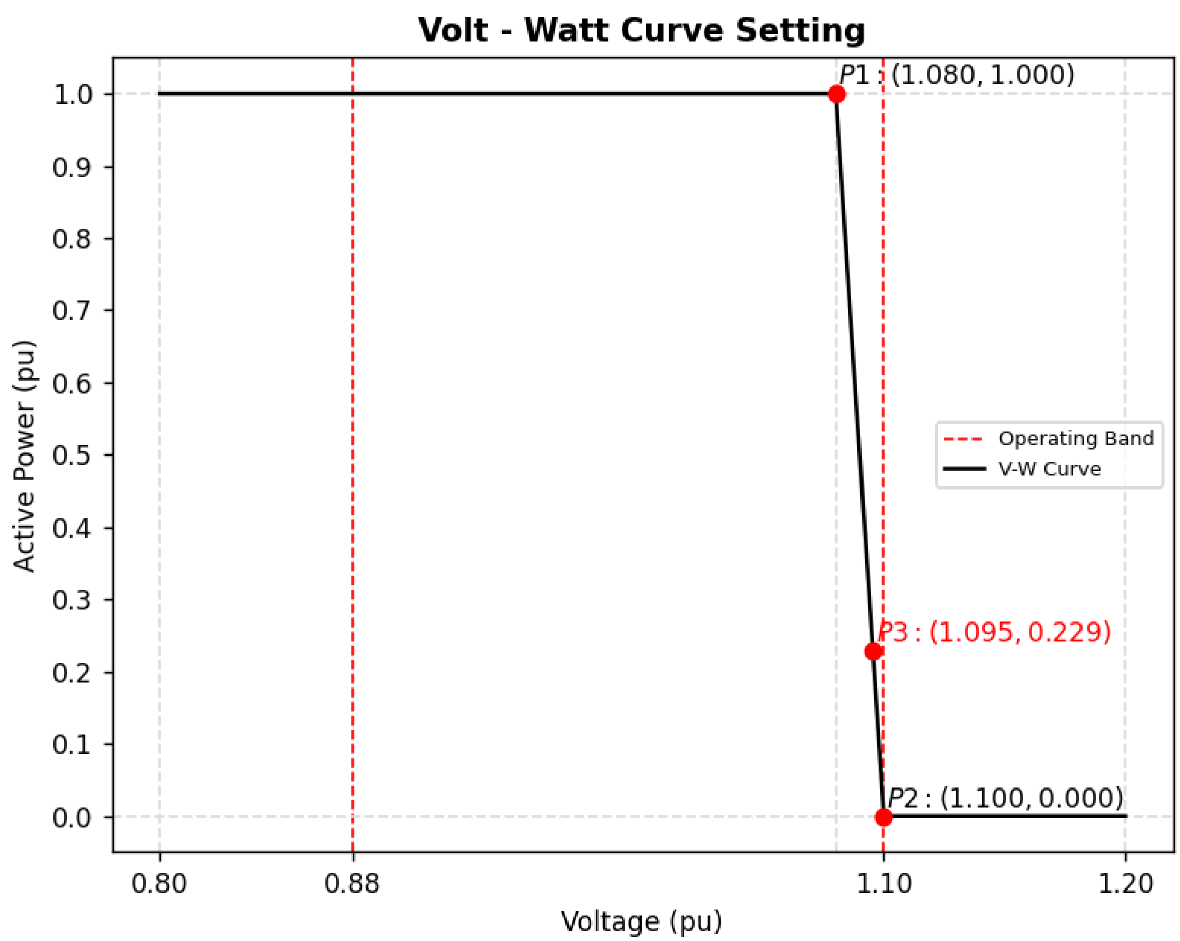

Note. Own elaboration.

On the other hand, Figure 3.7 displays the variables of the generator that experienced overvoltage, PVS 6. Point P_3, represents the voltage and power after incorporating the curve, and due to its the voltage exceed 1.08 pu, the power output should be reduced to 229 kW, as shown in the graph. However, the inverter can only produce up to 200 kW so the implemented programming will establish that maximum output power of the inverter.

3.2.2 Volt-var curve from the generation point of view

When the Volt-var curve mode was activated, the successful elimination of overvoltage was achieved through the absorption of reactive power from the grid. Nonetheless, the impact of this control resulted in the adjustment of the active power of all PV systems to maintain the apparent power at 1000 kVA. The following table shows what was indicated:

Table 33.2

Voltage, active and reactive power when the Volt-var curve are applied from the generation point of view

Node	**PVS**	**Voltage (pu)**		**Active Power (kW)**		**Reactive Power (kvar)**		**Power Factor**
		0 kW	1000 kW	0 kW	1000 kW	0 kW	1000 kW	1000 kW
840	1	1.0302	1.0660	0	1000	0	0	1
844	2	1.0306	1.0643	0	1000	0	0	1
848	3	1.0308	1.0665	0	1000	0	0	1
860	4	1.0305	1.0645	0	1000	0	0	1
816	5	1.0223	1.0494	0	1000	0	0	1
830	6	0.9954	1.1050	0	911	0	-440	0.910
858	7	1.0346	1.0495	0	1000	0	0	1

Note. Own elaboration.

The sixth PV system consumed the highest amount of reactive power and exhibited the lowest production, at 911 kW and PF. In general, these values are more acceptable from technical and economic perspectives, compared to the results obtained with the previous control.

To validate the proposed Volt-var graph configuration, two cases will be presented in which the curve will be displayed with maximum voltage when there is no overvoltage (PVS 2) and when there is overvoltage (PSV 6).

Figure 3.8

Graph of the Volt-var curve with voltage and output power of the PVS 2

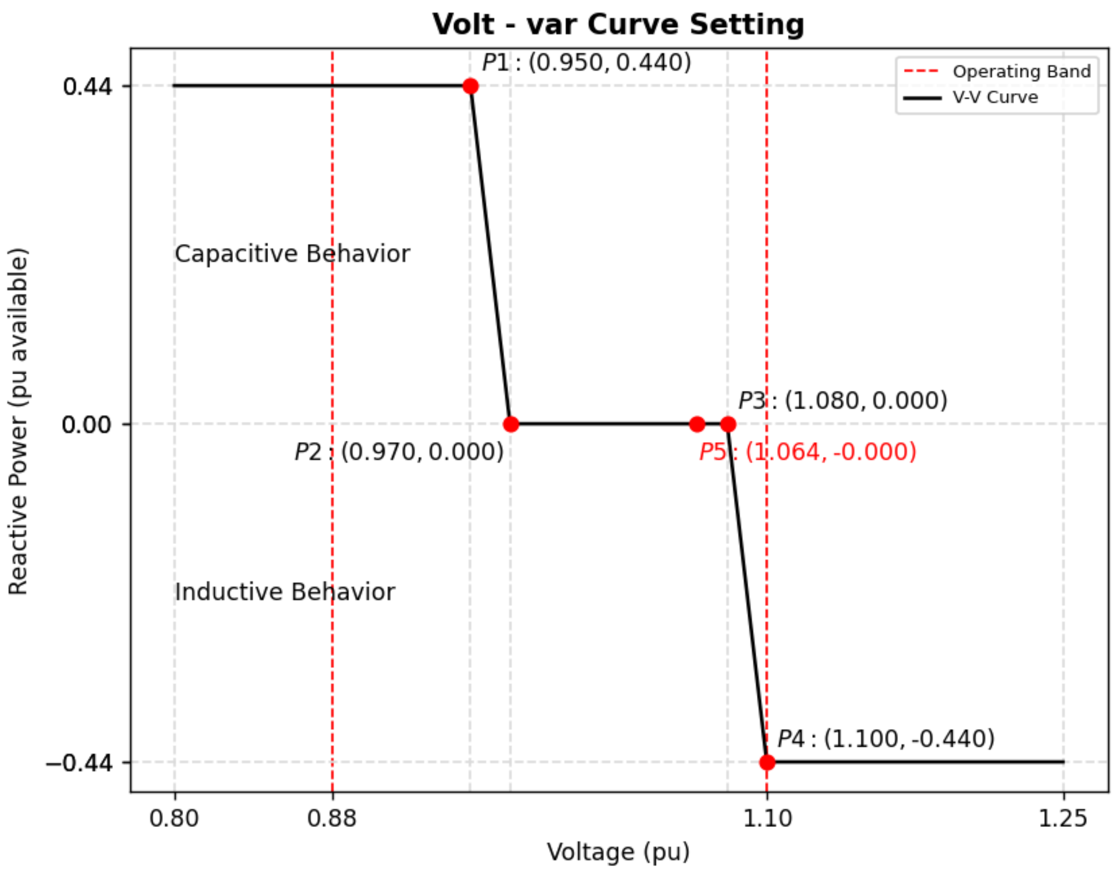

Note. Own elaboration.

As observed in the graph, when the highest irradiance occurs and does not exceed the voltage limit, point P_5 is located in the dead-band region. This means that the active power is at its maximum, and the reactive power is 0 kvar.

Figure 3.9

Graph of the Volt-var curve with voltage and output power of the PVS 6

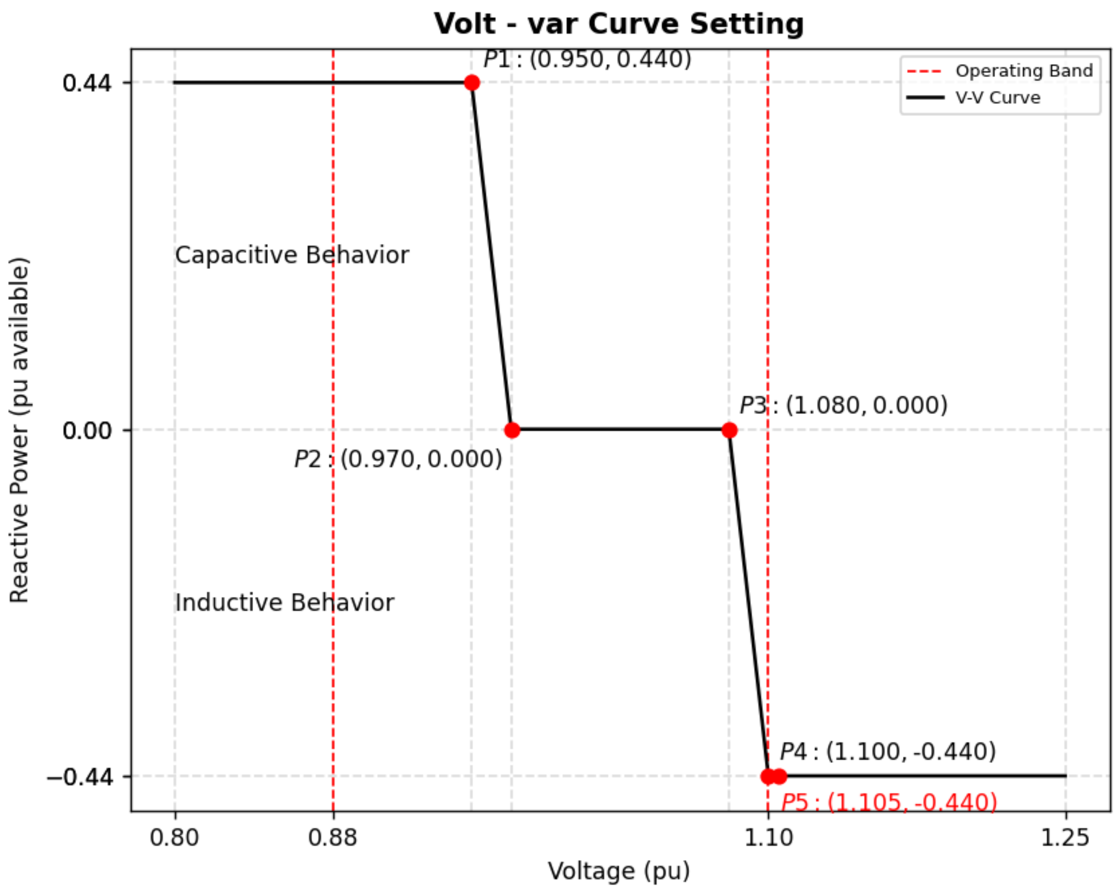

Note. Own elaboration.

The figure illustrates how PVS 6, which experienced overvoltage, required the absorption of 440 kvar of reactive power from the grid to decrease to a voltage level within the operational boundary of the network.

3.3 Results from the distribution point of view without voltage control

The continuous operation region established for this point of view was 1±0.5 pu, so the voltage curves in each of the PVS nodes shown in Figure 3.8 must respect this band. It should be noted that for this section the results for systems of 500 kW (broken lines) and 1000 kW (dotted lines) will be presented.

Figure 3.10

Voltages at the nodes of the PV units from the distribution point of view. a) Voltage of PVS 1, 2, 3 and 4 b) Voltage of PVS 5 c) Voltage of PVS 6 d) Voltage of PVS 7

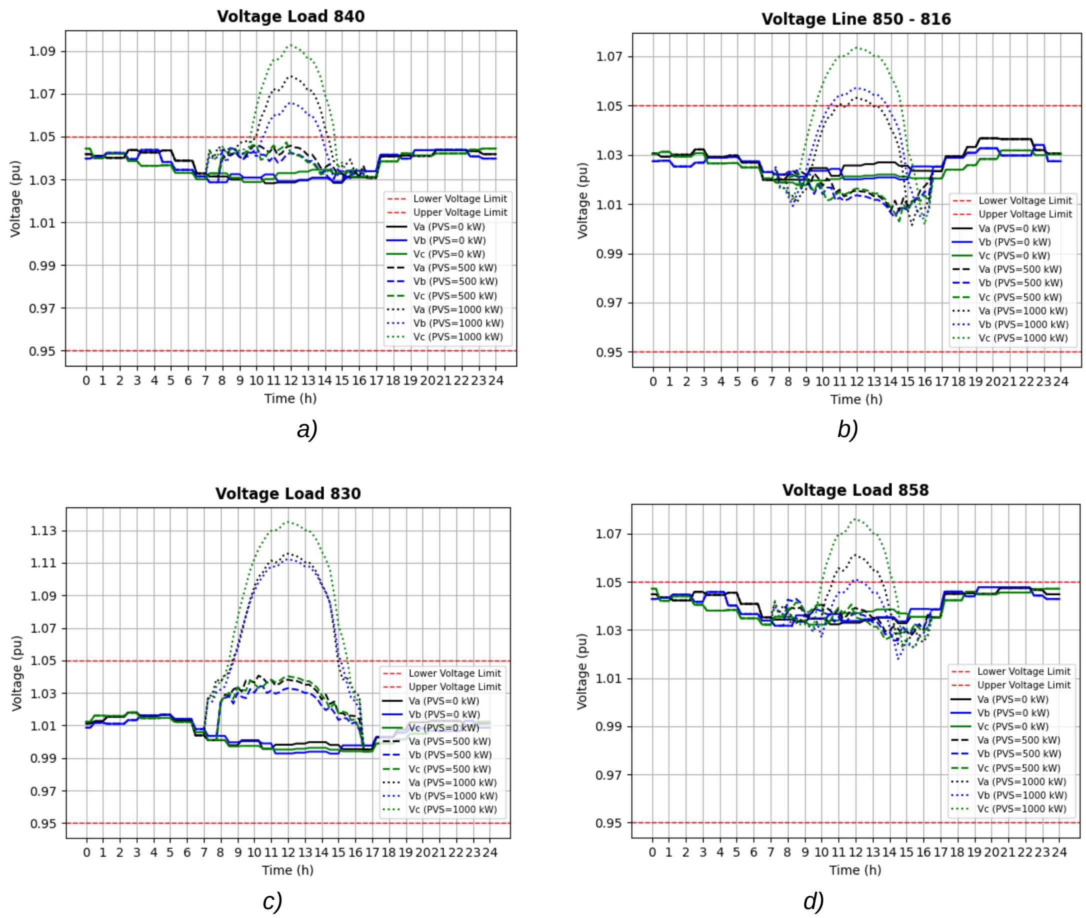

Note. Own elaboration.

All PVS at the distribution level with a capacity of 1000 kW, when operating simultaneously, experienced overvoltage. The spot with the highest voltage levels was node 830, where is connected the PVS 6. The following bar graph illustrates the steady state voltage problem.

Figure 3.11

Voltages for each photovoltaic system from the distribution point of view

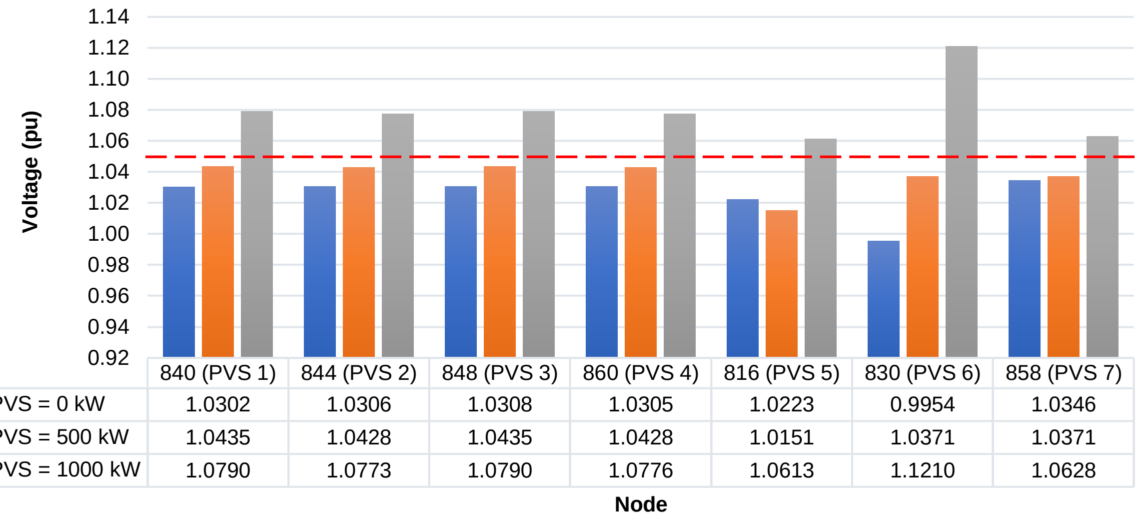

	840 (PVS 1)	844 (PVS 2)	848 (PVS 3)	860 (PVS 4)	816 (PVS 5)	830 (PVS 6)	858 (PVS 7)
PVS = 0 kW	1.0302	1.0306	1.0308	1.0305	1.0223	0.9954	1.0346
PVS = 500 kW	1.0435	1.0428	1.0435	1.0428	1.0151	1.0371	1.0371
PVS = 1000 kW	1.0790	1.0773	1.0790	1.0776	1.0613	1.1210	1.0628

Note. Own elaboration.

3.3.1 Volt-Watt curve from the distribution point of view

When this mode was activated, the voltage and power results were recorded to assess if there was a decrease in any of these variables. In the following graphs, there are three bars indicating the cases in which the method was used and not used: 'Without Curve 1' refers to the data of 500 kW PV systems, 'Without Curve 2,' and 'Volt-Watt curve' for 1000 kW PVS.

Figure 3.12

Voltage applying Volt-Watt curve from the distribution point of view

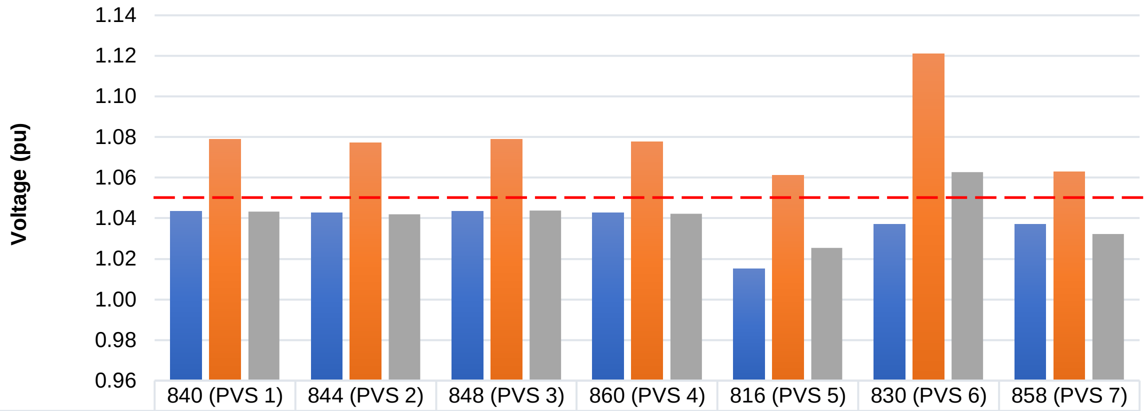

	840 (PVS 1)	844 (PVS 2)	848 (PVS 3)	860 (PVS 4)	816 (PVS 5)	830 (PVS 6)	858 (PVS 7)
Without Curve 1	1.0435	1.0428	1.0435	1.0428	1.0151	1.0371	1.0371
Without Curve 2	1.0790	1.0773	1.0790	1.0776	1.0613	1.1210	1.0628
Volt-Watt Curve	1.0432	1.0420	1.0437	1.0422	1.0253	1.0628	1.0322

Node

Note. Own elaboration.

Figure 3.13

Active Power applying Volt-Watt curve from the distribution point of view

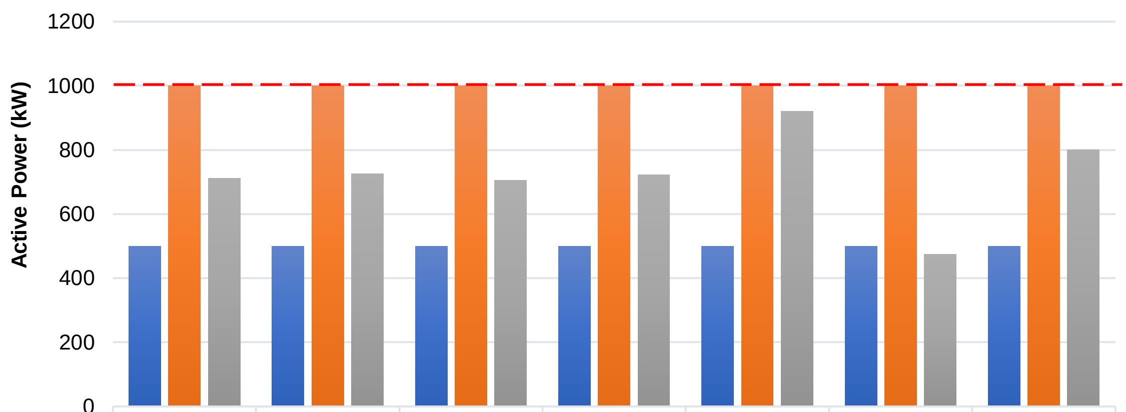

	840 (PVS 1)	844 (PVS 2)	848 (PVS 3)	860 (PVS 4)	816 (PVS 5)	830 (PVS 6)	858 (PVS 7)
Without Curve 1	500	500	500	500	500	500	500
Without Curve 2	1000	1000	1000	1000	1000	1000	1000
Volt-Watt Curve	712	725	706	723	920	474	800

Node

Note. Own elaboration.

In all cases the overvoltage was corrected, except for node 830 because its voltage went outside the band limit, and also its output power was 47.4% of what it should be. Therefore, to try to correct this, it was decided to reduce the capacity of the PVS 6 to 100 kW. The results of the power change were these:

Figure 3.14

Voltage applying Volt-Watt curve when PV Generator 6 has an output of 100 kW

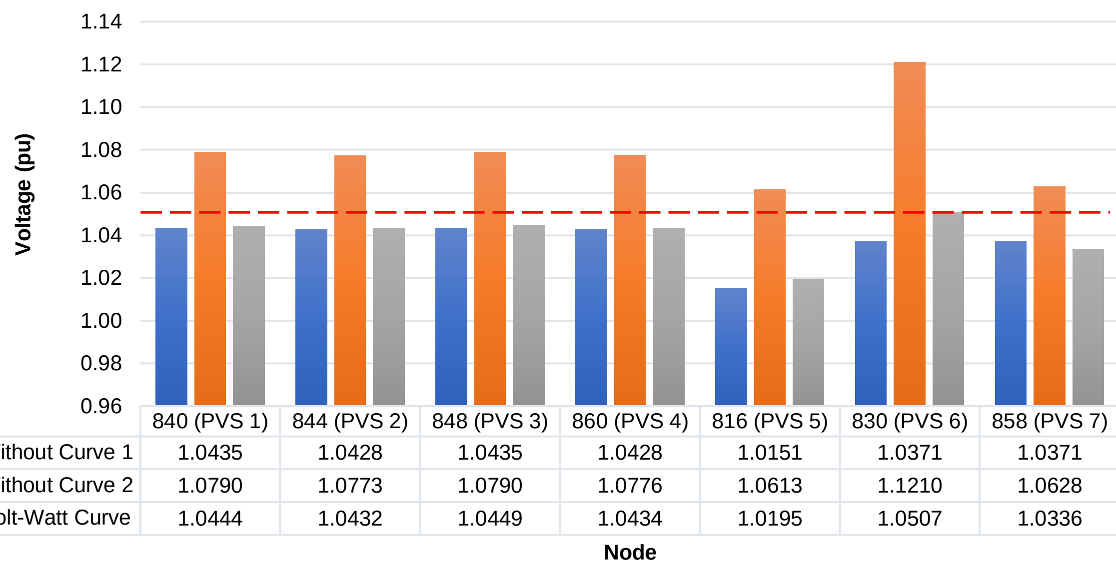

	840 (PVS 1)	844 (PVS 2)	848 (PVS 3)	860 (PVS 4)	816 (PVS 5)	830 (PVS 6)	858 (PVS 7)
Without Curve 1	1.0435	1.0428	1.0435	1.0428	1.0151	1.0371	1.0371
Without Curve 2	1.0790	1.0773	1.0790	1.0776	1.0613	1.1210	1.0628
Volt-Watt Curve	1.0444	1.0432	1.0449	1.0434	1.0195	1.0507	1.0336

Note. Own elaboration.

Figure 3.15

Power applying Volt-Watt curve when PV Generator 6 has an output of 100 kW

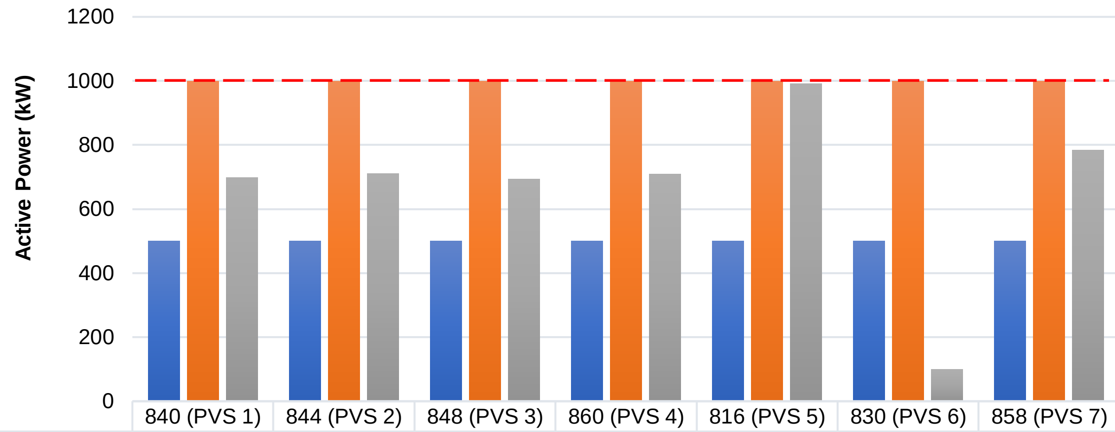

	840 (PVS 1)	844 (PVS 2)	848 (PVS 3)	860 (PVS 4)	816 (PVS 5)	830 (PVS 6)	858 (PVS 7)
Without Curve 1	500	500	500	500	500	500	500
Without Curve 2	1000	1000	1000	1000	1000	1000	1000
Volt-Watt Curve	699	711	693	710	992	100	784

Node

Note. Own elaboration.

With the decrease in the power of the sixth PV system and applying the Volt-Watt curve, it was observed that the voltage in the node was 1,057 and that the active output powers were lower than the results of the previous system. For example, PVS 7 had an output of 800 kW and with the change it was reduced to 784 kW.

To demonstrate that the configuration of the Volt-Watt curves was appropriate, Figure 3.13 and Figure 3.14 were plotted, illustrating the curve settings at maximum voltage produced at noon, along with the corresponding power output.

Figure 3.16

Graph of the Volt-Watt curve with voltage and output power of the PVS 5

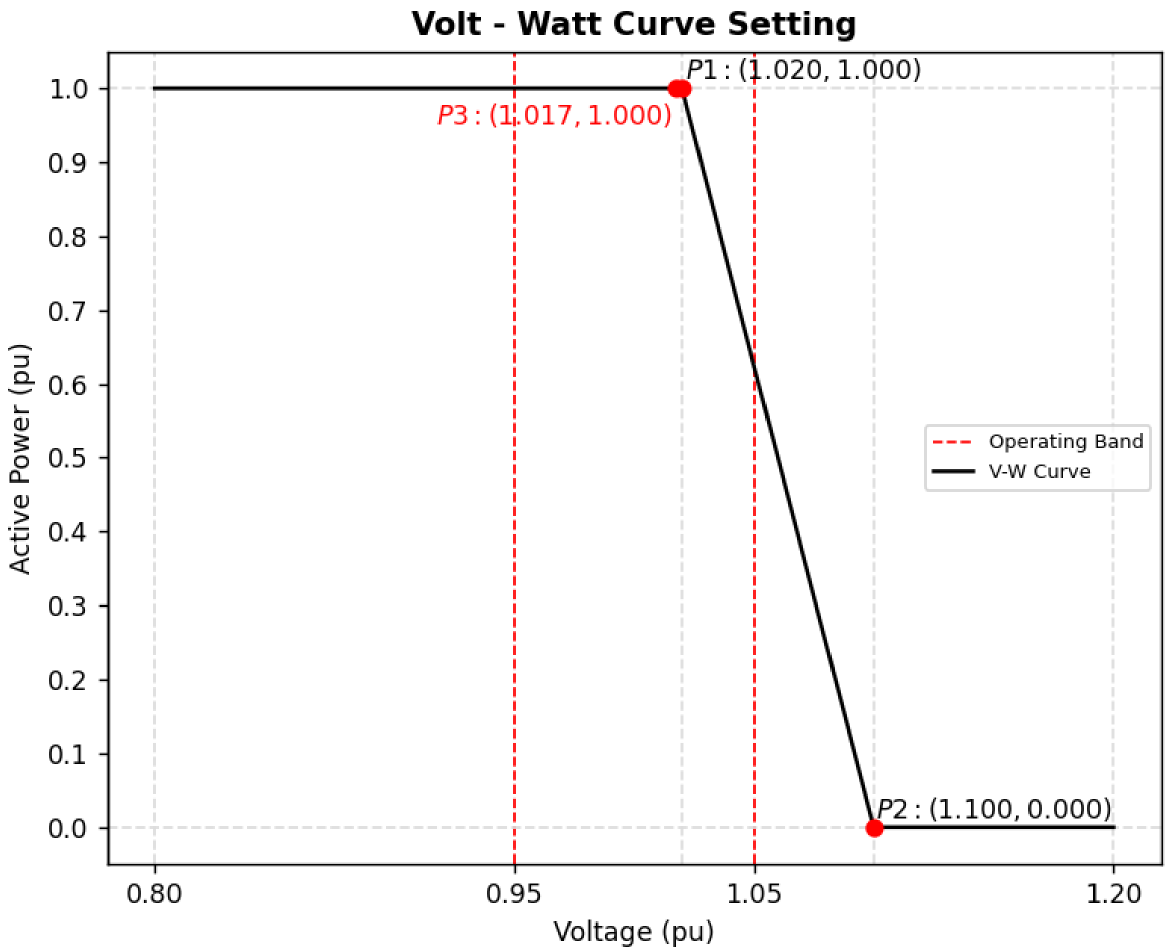

Note. Own elaboration.

Figure 3.14 specifically shows the variables of PVS 5, which is an example of a generator without overvoltage, and since its voltage is below 1.02 pu, the power output was at 1 pu (equivalent to 500 kW).

Figure 3.17

Graph of the Volt-Watt curve with voltage and output power of the PVS 6

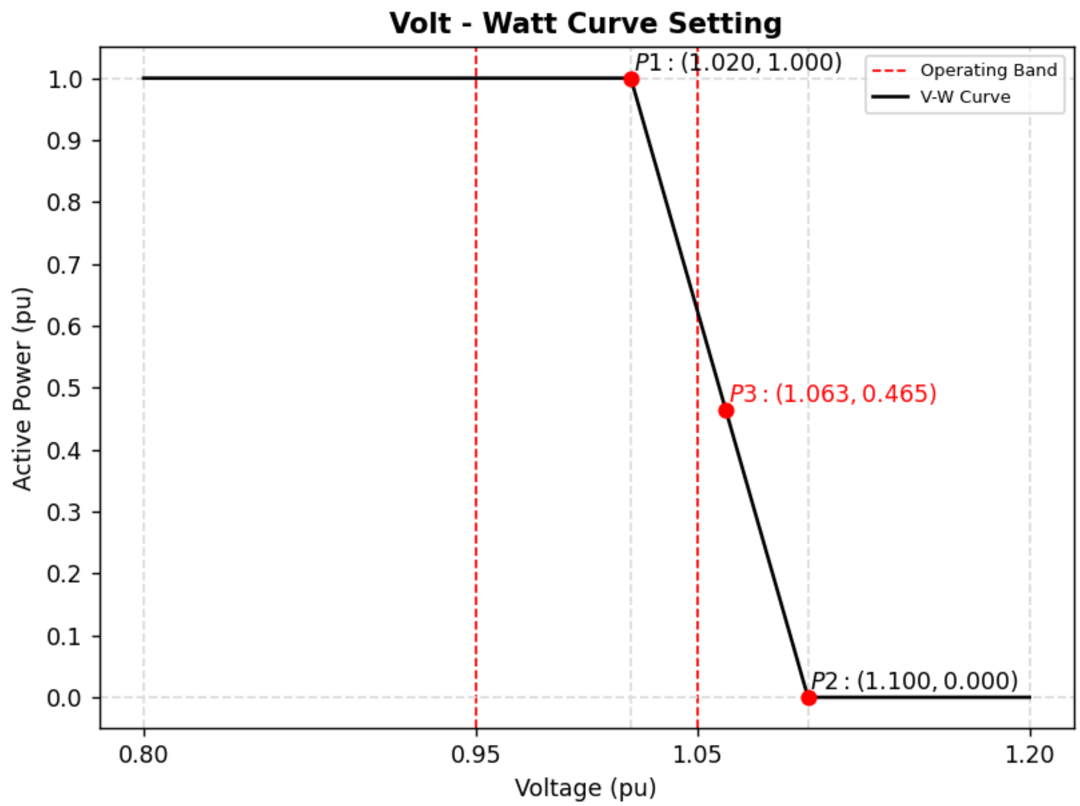

Note. Own elaboration.

On the other hand, Figure 3.15 displays the variables of the generator that experienced overvoltage, PVS 6. Point P_3, represents the voltage and power after incorporating the curve, and due to its the voltage exceed 1.02 pu, the power output should be reduced to 465 kW, as shown in the graph. However, the inverter can only produce up to 100 kW so the implemented programming will establish that maximum output power of the inverter.

3.3.2 Volt-var curve from the distribution point of view

When this mode began to work, it was observed that the overvoltage was mitigated through the absorption of a certain amount of reactants from the network. The results show that the active power output for each PVS was around nine hundred kilo-Watts onwards, which compared to the previous control shows that it is more effective in terms of releasing a greater amount of power.

For this control, the PVS at node 816 was the one that gave all its power output, and that at node 830 had the lowest output, 914 kW. In **¡Error! No se encuentra el origen de la referencia.** t he data of voltage, active and reactive power, and power factor of each photovoltaic unit were recorded.

Table 3.3

Voltage, active and reactive power when the Volt-var curve are applied from the distribution point of view

Node	PVS	Voltage (pu)			Active Power (kW)		Reactive Power (kvar)	Power Factor
		0 kW	500 kW	1000 kW	0 kW	1000 kW	1000 kW	1000 kW
840	1	1.0302	1.0435	1.0459	0	925	-380	0.925
844	2	1.0306	1.0428	1.0447	0	932	-363	0.932
848	3	1.0308	1.0440	1.0464	0	922	-388	0.922
860	4	1.0305	1.0428	1.0449	0	931	-365	0.931
816	5	1.0223	1.0151	1.0095	0	1000	0	1
830	6	0.9954	1.0371	1.0478	0	914	-406	0.914
858	7	1.0346	1.0371	1.0345	0	965	-263	0.965

Note. Own elaboration.

To validate the proposed Volt-var graph configuration, two cases will be presented in which the curve will be displayed with maximum voltage when there is no overvoltage (PVS 5) and when there is overvoltage (PSV 6).

Figure 3.18

Graph of the Volt-var curve with voltage and output power of the PVS 5

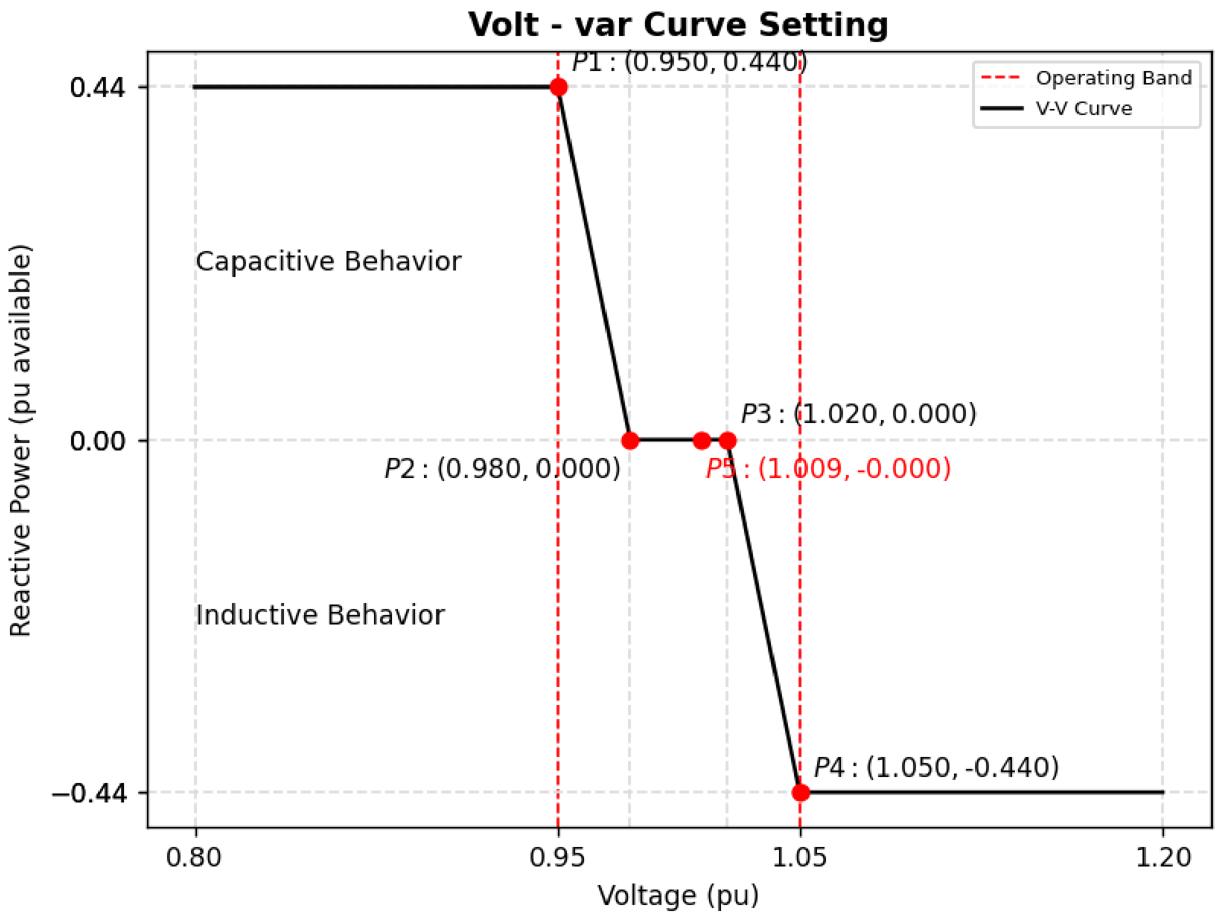

Note. Own elaboration.

As observed in the graph, when the highest irradiance occurs and does not exceed the voltage limit, point P_5 is located in the dead-band region. This means that the active power is at its maximum, and the reactive power is 0 kvar.

Figure 3.19

Graph of the Volt-var curve with voltage and output power of the PVS 6

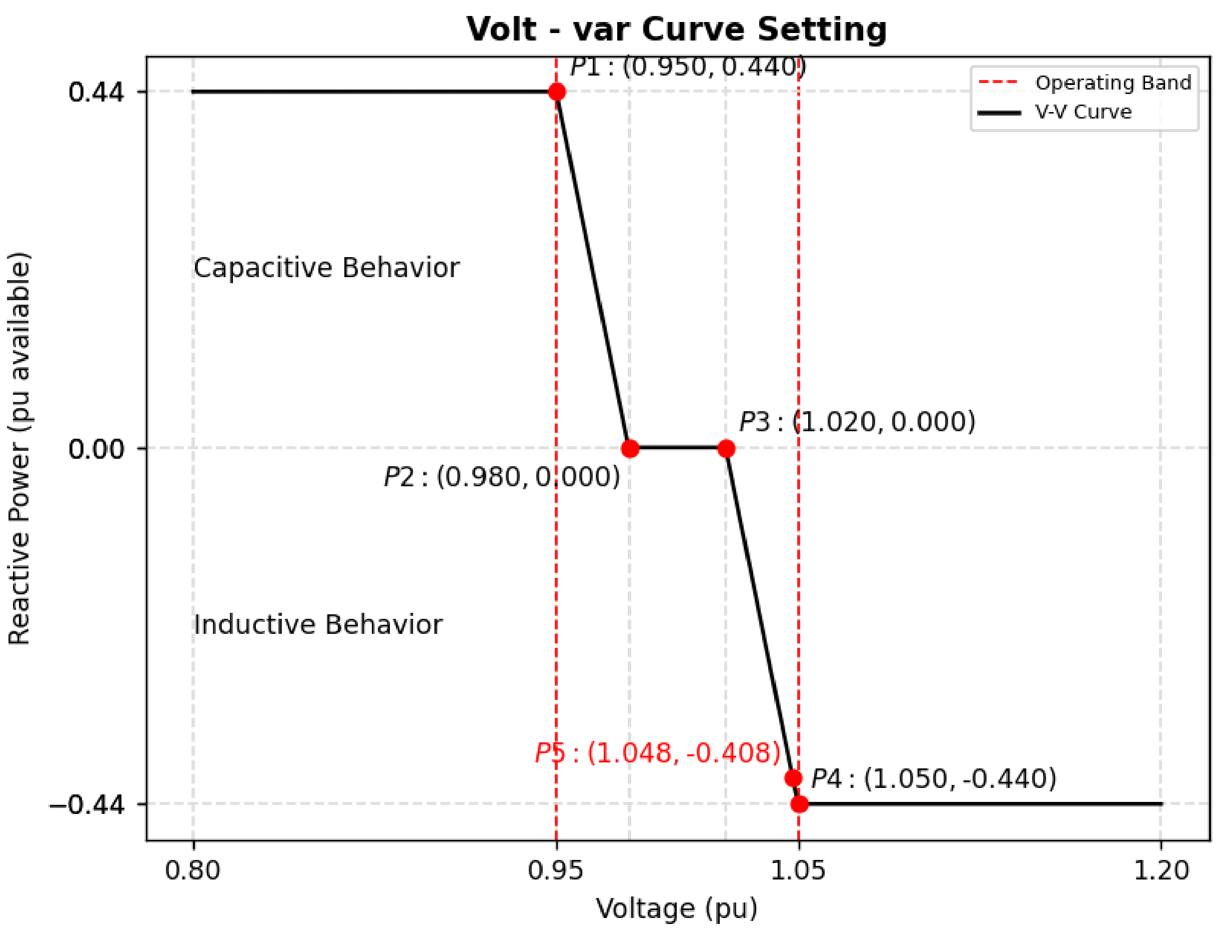

Note. Own elaboration.

The figure illustrates how PVS 6, which experienced overvoltage, required the absorption of 408 kvar of reactive power from the grid to decrease to a voltage level within the operational band.

3.4 Analysis of results

In this section, the analysis of the results will be conducted from the perspectives of generation and distribution.

3.4.1 Generation point of view

For this perspective, seven photovoltaic generators with a maximum capacity of 1000 kW were installed at different spots to observe the consequences on the voltage resulting from the large accommodation of PVS into a distribution network. Initially, when the photovoltaic DERs were not installed, the voltage behaved in accordance with the continuous line in Figure 3.1, within the continuous operation band. However, upon activation of all PV systems, a significant increase in voltage was observed, with one of them (PVS 6) experiencing an average overvoltage of 2.10% above the upper band. This primarily occurs due to the power disparity between generation and the capacity that can be connected at a node or bus before encountering issues related to energy quality.

Generally, to address faults or contingencies that occurred, the same network protection elements were used such as voltage regulators, shunt capacitors, tap-changing transformers, and others. Nevertheless, with the inclusion of DERs certain fault events have not been covered. As a result, voltage regulation modes such as Volt-Watt and Volt-var curve, have been incorporated into the intelligent inverters of PVS.

When the Volt-Watt curve control was applied, it was observed that the overvoltage was mitigated, but the power output of the sixth generator drastically decreased to 231 kW, significantly below the outputs of the other generators. In an effort to maintain a scenario where all power outputs are at their maximum, the decision was made to reduce the output of Generator 6 to 200 kW. This adjustment ensures that all systems, applying the Volt-Watt curves, can eliminate overvoltage while operating at their maximum generation capacity, as illustrated in Bar Chart Figure 3.5.

On the other hand, the Volt-var curve control for generation proved to be more effective, as its operation did not require changes or requests for a unit to decrease its generation by 20%. Overvoltage was eliminated by absorbing reactive power from the grid at its Point of Common Coupling (PCC). The greatest amount of reactive power consumed was by PVS 6 (440 kvar), resulting in a reduction in voltage from 1.1210 to 1.105 per unit. In contrast, the other systems, not experiencing overvoltage, the Volt-var curve control didn't allow reactive power absorption at the PCC. It is important to highlight that this control, due to its configuration, has a maximum limit for injecting and absorbing of 440 kvar. Therefore, if the overvoltage is sufficiently high to prevent it from decreasing to a value below 1.10 pu with the control, then the control will be inefficient, as it will consume all the available reactive power, exceeding the voltage limit of the operational band.

Figure 3.20

Active power in absence and application of regulation curves, from the generation perspective

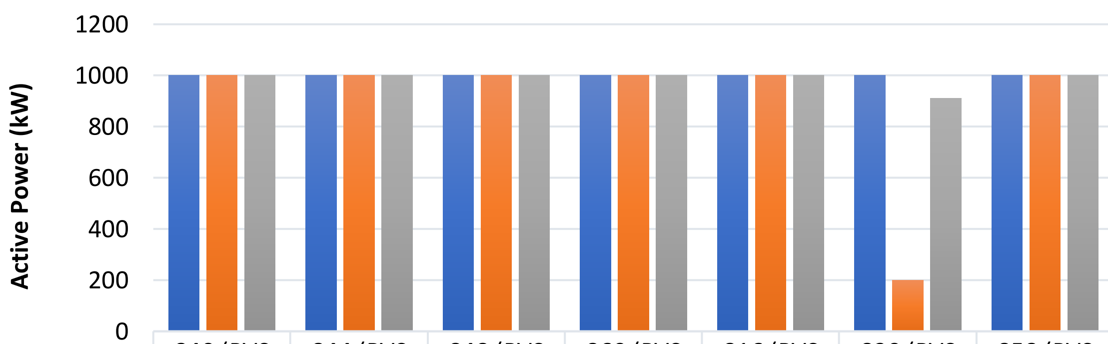

	840 (PVS 1)	844 (PVS 2)	848 (PVS 3)	860 (PVS 4)	816 (PVS 5)	830 (PVS 6)	858 (PVS 7)
Without Curves	1000	1000	1000	1000	1000	1000	1000
Volt-Watt Curve	1000	1000	1000	1000	1000	200	1000
Volt-var Curve	1000	1000	1000	1000	1000	911	1000

Node

Note. Own elaboration.

Each type of control has its own impact that can appropriately benefit the network. Volt-Watt curve control mitigates voltage issues under steady-state conditions but reduces at least one of the output powers to a considerably low value, resulting in economic losses for the generator, which has its equipment designed to produce a other amount of energy. Meanwhile, Volt-var curve control for this kind of network provides a quick response to prevent exceeding the upper limit of the voltage band by absorbing a specific amount of reactive power, albeit with a 9% reduction in the output power of generator 6, which is the most affected.
It can be added that these two methods, especially Volt-var for medium-voltage networks, can be valuable for conducting an analysis of large photovoltaic systems and providing an estimate of generation capacity when aiming to maximize photovoltaic production.

3.4.2 Distribution point of view

The implementation of the Volt-Watt and Volt-var regulation curves were also carried out from the distribution point of view. The standard used as a basis to determine when a voltage limit violation occurs is ANSI C84.1 – 2020, which establishes that the operating band should be between 0.95 and 1.05 in per unit. Additionally, to assess the voltage effects of accommodating PVS into the network, three scenarios were tested. The first scenario represents the absence of any photovoltaic generation, while the second and third scenarios involve the integration of photovoltaic systems with capacities of 500 kW and 1000 kW, respectively.

In light of the foregoing, the simulation of the IEEE 34-bus feeder was made without any regulation curves. It was found that for the scenarios of 0 kW (without photovoltaic integration) and 500 kW, the voltage is within the operating band, indicating that the network's hosting capacity can easily accommodate this level of photovoltaic penetration. Nonetheless, when the distribution system includes units of 1000 kW, the voltage scenario changes dramatically, as depicted in Figure

3.9 The photovoltaic systems cause an increase in voltage above 1.05 pu at all seven PCCs. Quantifying this data reveals that nodes 816 and 830 exhibit the lowest and highest voltage violation levels, with values of 1.06 and 1.12 per unit, respectively. Consequently, this results in a deterioration of power quality and a limitation in the hosting capacity of the feeder.

First, the implementation of the Volt-Watt curves applied to each PVS in the case study will be analyzed, with each setting based on IEEE Standard 1547. The simulation was made for the three scenarios, this time focusing on the 1000 kW case, as it involves a transgression of the voltage limit. The results upon applying the curve were that in almost all nodes, overvoltage was eliminated, with an average output power of 764 kW, as observed in Figure 3.11 This in comparison to the scenario without regulation curves, represents a power loss of 23.6%. Node 830 was the exception in voltage mitigation as despite the application of curves, they were not sufficiently effective in reducing the voltage within the operating range. It reached 1.06 per unit, with an output power of 474 kW, representing a capacity loss of 52.6%. For this reason, the production of PVS 6 was limited to 100 kW, as shown in Figure 3.13. This adjustment allowed the reduction of overvoltage across all PCCs and staying within operational limits to enhance the power quality of the network. It is important to note that the decision to decrease the capacity of PVS 6 to a value below 500 kW was motivated by the fact that, in the 1000 kW scenario, there is an additional 500 kW from the seven generators that works at the same capacity simultaneously. Therefore, applying curve control leads to a more significant impact on power when attempting to compensate for voltage increases. Reducing the capacity of one generator to 500 kW in the case of a 1 MW scenario may not necessarily yield optimal results, as adjusting power levels in one spot affects the Power and Voltage of other nodes. After several tests, it was concluded that reducing the power of PVS 6 to 100 kW was the most viable option.

The second proposal used to mitigate overvoltage is the Volt-var curve, configured in accordance with IEEE standard 1547. Once again, the three scenarios were simulated, with a focus on the analysis of 1000 kW photovoltaic penetration. The results of applying the control kept the voltage below the upper limit of the band (1.05 per unit). Additionally, the power output for each of the PV system units averaged 941 kW, as detailed in **¡Error! No se encuentra el origen de la referencia.**, representing an average loss of 5.9% compared to the maximum generation when there are no regulation curves. The reduction in overvoltage and the change in power output are attributed to the method, as the control decreases overvoltage by absorbing reactive power from the network at the PCC. Furthermore, it can be stated that the most critical case is node 830 because it required the absorption of the highest amount of reactive power, 406 kvar. Hence, the use of the Volt-var curve allows for the reduction of overvoltage, leading to a decrease in output power by an average of 59 kW for each of the photovoltaic units.

Figure 3.21

Active power in absence and application of regulation curves, from the distribution perspective

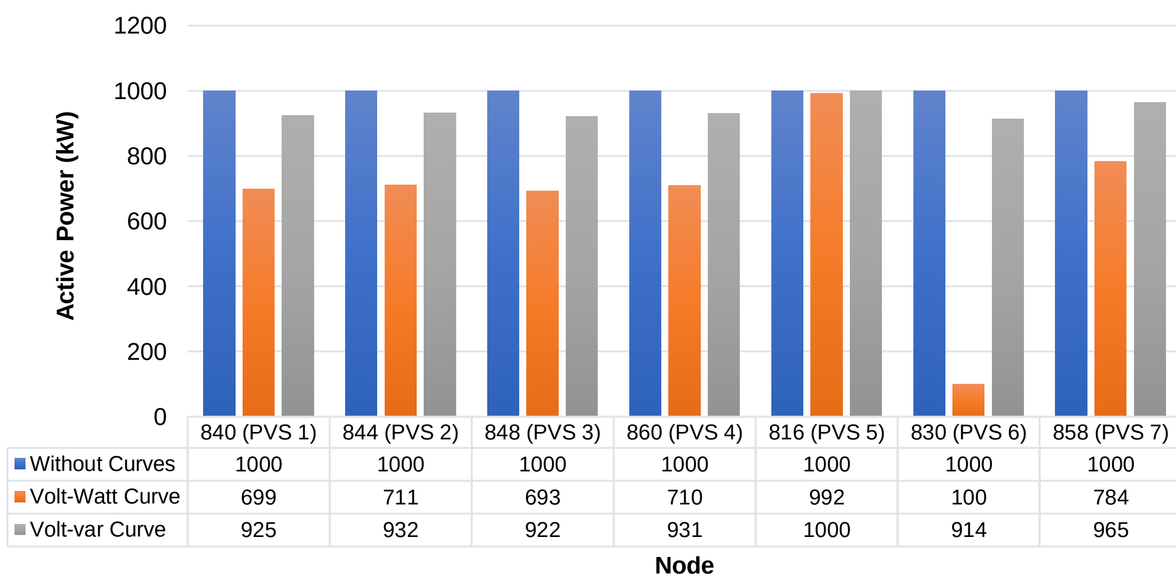

Note. Own elaboration.

Both methods for protecting the system from voltage issues are viable from a distribution point of view, but the Volt-var curve are more efficient in controlling overvoltage and increasing the network's hosting capacity. This assertion is justified by the analysis conducted on node 830 because, in the case of Volt-Watt curve control, it was necessary to reduce the capacity of PVS 6 to 100 kW to avoid violating the voltage limit. However, it is noteworthy that in this node, with the implemented change, the voltage level was not reduced within the bounds of the ANSI C84.1 – 2020 standard. Decreasing photovoltaic production and having surges from a power quality perspective is very risky due to the weakness of distribution networks. In contrast, the Volt-var curve present a more efficient control because, for the same node and all PV systems, without making any modifications, the steady-state voltage issue was mitigated, and more than 90% of power was generated. The results of the study node using the curves are 1.04 pu for the voltage and output power of 914 kW; in **¡Error! No se encuentra el origen de la referencia.**, the before and after applying the curve to these variables can be visualized.

Therefore, the Volt-var curve for the distribution point of view present more advantages than the other method because there was greater production in the PV systems and elimination of overvoltage. Besides, it can be said that this control is a viable alternative for equipment that is unable to mitigate the rapid fluctuation of voltage levels that occur due to photovoltaic systems, either due to changing irradiance or when photovoltaic generation is too high and the load is very low.

Chapter 4

4.1 Conclusions and recommendations

In this section, the conclusions of the investigation into the impact of regulation curves on an IEEE distribution system will be listed. Moreover, the observed recommendations throughout the project will be mentioned with the explicit intention of refining and optimizing the employed controls.

4.1.1 Conclusions

- It was analyzed and compared the impact of regulation curves for the selected medium-voltage distribution system. The Volt-var curve showed a better impact for the two chosen perspectives, eliminating overvoltage and ensuring that the power output did not decrease by more than 8.9% for generation and 8.6% for distribution. On the other hand, the Volt-Watt curves eliminated overvoltage but reduced the active power output of one of the PVS to 20% and 10% of its production, respectively. Nevertheless, like the Volt-var curve, it's a valuable method for analyzing photovoltaic systems and providing an estimation of generation capacity, but depending on the type of network and its X/R ratio.
- The IEEE 34-bus distribution network was selected for conducting tests with seven Photovoltaic Systems placed at different nodes. The results indicated that there are steady-state voltage issues when all the PVS are 1000 kV at the PCC, for both perspectives of the study. Node 830 was the most adversely affected, its average voltage reaches to 1.12 pu. To address this, voltage regulation curves were independently applied to assess their impact on voltage reduction and active power output.
- Prior to the implementation of regulation curves, during the placement of 500 and 1000 kW photovoltaic systems on the 34-bus feeder, it was evident that carrying out proper planning regarding the identification of locations causing minimal deterioration in energy

quality is crucial for the network. Based on this, the implementation of regulation curves and adequate planning for the placement of PV units can lead to preventing the infringement of network hosting capacity, thereby guaranteeing compliance with the continuous operation limits specified by the ANSI C84.1 – 2020 and IEEE 1547™ - 2018 standards.

- The results obtained in the output power curve of PV System 6 from both perspectives when Volt-Watt curves are applied are attributed to the fact that the node (830) to which this PV system is connected undergoes the changes. In other words, it acts as a slack bus, absorbing the higher impact of power reduction so that the other spots exhibit improved behavior in their variables. For this reason, it was decided to decrease the power output of PV System 6 to prevent having a low plant capacity factor compared to the other units.
- Installing a large number of PVSs in the network also entails the installation of a significant number of smart inverters, which induce to problems in the power quality of the network due to the electronic components with which they are manufactured. This becomes more evident at nodes, especially in the case of 1000 kW photovoltaic systems, as the voltage signals that are in phase when there is no distributed generation, end up exhibiting an imbalance between phases. Consequently, the electronic components that make up the inverter contribute to a distortion in the voltage wave.
- It was determined that the smart inverter, in order to decrease the power output of the photovoltaic units, use the average voltage of lines A, B, and C. Therefore, the application of regulation curves on an unbalanced network becomes more complex than on a balanced network, such as the case of the IEEE 34-Bus feeder.

- It has been identified that Volt-var control does not incur significant technical and economic losses compared to Volt-Watt curves. Therefore, for this case study, Volt-var curve are deemed the most efficient method. Furthermore, they enable higher attainment of plant capacity factor, revenue generation, and quick return on investment compared to the other method.

4.1.2 Recommendations

- Combine Volt-Watt and Volt-var curve controls to leverage the benefits of each. In other words, implement a control system that enables the elimination of overvoltage while maximizing energy production to the greatest extent possible.
- It is advisable to use real data for the irradiance factor curve to approximate the results of the case study with reality, as this variable is influenced by cloud movement.
- It is recommended to review the power factor limits of the PVS inverter for the setting of the reactive power limits in the Volt-var curve.
- When setting the Volt-var curve, it is recommended to simulate the regulation curve and the output voltage at different levels of PVS power output on the same graph. This allows identifying the intersection point of the output power and its voltage, allowing the curve configuration to be carried out appropriately and in accordance with the IEEE 1547™ - 2018 standard.
- Currently, there is no book where information on the behavior of regulation curves can be found. However, for those seeking a deeper understanding, it is recommended to read "Power System Stability & Control" by Prabha Kundur because this book can relate some concepts with the curves used.

References

[1] J. Roca, "El consumo eléctrico mundial crece más rápido que la población," *El periodico de la energía,* 2020.

[2] International Renewable Energy Agency, "Renewable Capacity Statistic 2023," 2023. [Online]. Available: https://mc-cd8320d4-36a1-40ac-83cc-3389-cdn-endpoint.azureedge.net/-/media/Files/IRENA/Agency/Publication/2023/Mar/IRENA_RE_Capacity_Statistics_2023.pdf?rev=d2949151ee6a4625b65c82881403c2a7.

[3] K. Alboaouh and S. Mohagheghi, "Voltage, var and watt optimization for a distribution system with high PV penetration: A probabilistic study," *Electric Power Systems Research,* 2019.

[4] T. Gönen, Electric Power Distribution System Engineering, McGraw-Hil, 1986.

[5] A. J. Harger, V. C. Cunha, L. Hernandes, F. Trindade, W. Freitas and H. O. Vilibor, "Avaliação do Impacto de Curvas Volt-Watt e Volt-var na Capacidade de Hospedagem de Microgeração Solar em Sistemas de Distribuição," *Conferência Brasileira Sobre Qualidade Da Energia Elétrica – Cbqee,* 2023.

[6] M. U. Hashmi, D. Deka, A. Bušic and D. Van Hertem, "Can locational disparity of prosumer energy optimization due to inverter rules be limited?," *IEEE Transactions on Power Systems,* 2022.

[7] K. Alboaouh and S. Mohagheghi, "Voltage, var and watt optimization for a distribution system with high PV penetration: A probabilistic study," *Electric Power Systems Research,* vol. CLXXX, no. 106159, pp. 1-4, 2020.

[8] G. K. Ari and Y. Baghzouz, "Impact of high PV penetration on voltage regulation in electrical distribution systems," *International Conference on Clean Electrical Power (ICCEP),* no. 744-748, 2011.

[9] J. M. Sexauer and . S. Mohagheghi, "Voltage Quality Assessment in a Distribution System With Distributed Generation—A Probabilistic Load Flow Approach," *IEEE Transactions on Power Delivery,* vol. XXVIII, no. 3, pp. 1652-1662, 2013.

[10] Y. Y. Adajah, S. Thomas, M. S. Haruna and S. O. Anaza, "Distributed Generation (DG): A Review," in *2021 1st International Conference on Multidisciplinary Engineering and Applied Science (ICMEAS)*, Abuja, 2021.

[11] N. Jenkins, R. Allan, P. Crossley, D. Kirschen and G. Strbac, Embedded generation, United Kingdom: The Institution of Electrical Engineers, 2000.

[12] M. Funsho Akorede, H. Hizam and E. Pouresmaeil, "Distributed energy resources and benefits to the environment," *Renewable and Sustainable Energy Reviews,* vol. 14, no. 2, pp. 724-734, 2010.

[13] IEEE Standard Association, "IEEE Standard for Interconnection and Interoperability of Distributed Energy Resources with Associated Electric Power Systems Interfaces," IEEE Standards Coordinating Committee 21 on Fuel Cells, Photovoltaics, Dispersed Generation, and Energy Storag, New York, 2018.

[14] L. Nousiainen, J. Puukko, . A. Maki, T. Messo, J. Huusari, J. Jokipii, J. Viinamaki, D. Torres Lobera, . S. Valkealahti and T. Suntio, "Photovoltaic Generator as an Input Source for Power Electronic Converters," *IEEE Transactions on Power Electronics,* vol. 28, no. 6, 2013.

[15] B. Arbab Zavar, E. Palacios Garcia, J. Vasquez and J. Guerrero, "Smart Inverters for Microgrid Applications: A Review," *Energies 2019,* vol. 12, no. 5, p. 840, 2019.

[16] D. Almeida, J. Pasupuleti, S. K. Raveendran y R. Basir Khan, «Performance Evaluation of Solar PV Inverter Controls for Overvoltage Mitigation in MV Distribution Networks,» *Electronics,* p. 10, 2021.

[17] M. M. d. A. Garcia, "Mitigação De Sobretensão Causada Pela Geração Fotovoltaica Com Técnicas Controle Volt-Var E Volt-Watt," *Revista de Engenharia e Tecnologia,* vol. XIV, no. 2, 2022.

[18] IEEE, "IEEE PES Test Feeder," IEEE, 17 September 2010. [Online]. Available: https://cmte.ieee.org/pes-testfeeders/resources/. [Accessed 1 January 2024].

[19] Electric Power Research Institute, "OpenDSS PVSystem Element Model," EPRI, 2011.

[20] ARCERNNR, "La ARCERNNR expide normativa de generación distribuida para el autoabastecimiento de consumidores regulados de energía eléctrica," ARCERNNR, 15 November 2023. [Online]. Available: https://www.controlrecursosyenergia.gob.ec/la-arcernnr-expide-normativa-de-generacion-distribuida-para-el-autoabastecimiento-de-consumidores-regulados-de-energia-electrica/. [Accessed 1 January 2024].

[21] ARCERNNR, "RESOLUCIÓN Nro. ARCERNNR-031/2023 - REGULACIÓN Nro. ARCERNNR-008/23," Gobierno del Ecuador, Quito, 2023.

[22] American National Standards Institute, "ANSI C84.1-2020: Electric Power Systems Voltage Ratings (60 Hz)," American National Standards Institute, United States, 2020.

[23] Corporate Finance Institute, "Net Present Value (NPV)," 2018. [Online]. Available: https://corporatefinanceinstitute.com/resources/valuation/net-present-value-npv/.

[24] Wall Street Prep, "Net Profit Margin - Guide to Understanding the Net Profit Margin," 2022. [Online]. Available: https://www.wallstreetprep.com/knowledge/net-profit-margin/.

[25] Indeed Editorial, "Cost Revenue Ratio: Definition and How To Calculate," January 2023. [Online]. Available: https://www.indeed.com/career-advice/career-development/cost-revenue-ratio.

Appendix A

Annex 1

Parameters of overhead line for IEEE- 34 Node Test Feeder

Line code	Phasing	Phase conductor ACSR	Neutral conductor ACSR	Spacing ID
300	B A C N	1/0	1/0	500
301	B A C N	#2 - 6/1	#2 - 6/1	500
302	A N	#4 - 6/1	#4 - 6/1	510
303	B N	#4 - 6/1	#4 - 6/1	510
304	B N	#2 - 6/1	#2 - 6/1	510

Note. Data taken from Distribution System Analysis Subcommittee - IEEE 34 Node Test Feeder (2017).

Annex 2

Length and parameters of line segments

Node A	Node B	Length (ft)	Line Code
800	802	2580	300
802	806	1730	300
806	808	32230	300
808	810	5804	303
808	812	37500	300
812	814	29730	300
814	850	10	301
816	818	1710	302

816	824	10210	301
818	820	48150	302
820	822	13740	302
824	826	3030	303
824	828	840	301
828	830	20440	301
830	854	520	301
832	858	4900	301
832	888	0	XFM-1
834	860	2020	301
834	842	280	301
836	840	860	301
842	844	1350	301
844	846	3640	301
846	848	530	301
850	816	310	301
852	832	10	301
854	856	23330	303

854	852	36830	301
858	864	1620	302
858	834	55830	301
860	836	2680	301
862	838	4860	304
888	890	10560	300

Note. Data taken from Distribution System Analysis Subcommittee - IEEE 34 Node Test Feeder (2017).

Annex 3

Transformer Data

Transformer	Capacity (kVA)	kV-High	kV-Low	R %	X %
Main transformer (Substation)	2500	69 - D	24.9 – Gr. Y	1	8
XFM -1	500	24.9 – Gr.W	4.16 – Gr.W	1.9	4.08

Note. Data taken from Distribution System Analysis Subcommittee - IEEE 34 Node Test Feeder (2017).

Annex 4

Capacitor Data

Node	Phase A (kVAr)	Phase B (kVAr)	Phase C (kVAr)
844	100	100	100
848	150	150	150
Total	250	250	250

Note. Data taken from Distribution System Analysis Subcommittee - IEEE 34 Node Test Feeder (2017).

Annex 5

Setting of voltage regulator 1

Regulator ID	1		
Line Segment	814 - 850		
Phases	A - B - C		
Monitoring Phase	A - B - C		
Bandwidth	2.0 Volts		
PT Ratio	120		
Primary CT Rating	100		
Compensator Settings	Phase A	Phase B	Phase C
R – Setting	2,7	2,7	2,7
X – Setting	1,6	1,6	1,6
Volltage Level	122	122	122

Note. Data taken from Distribution System Analysis Subcommittee - IEEE 34 Node Test Feeder (2017).

Annex 6

Setting of voltage regulator 2

Regulator ID	2		
Line Segment	852 – 832		
Phases	A - B - C		
Monitoring Phase	A - B - C		
Bandwidth	2.0 Volts		
PT Ratio	120		
Primary CT Rating	100		
Compensator Settings	Phase A	Phase B	Phase C
R – Setting	2,5	2,5	2,5
X – Setting	1,5	1,5	1,5
Volltage Level	124	124	124

Note. Data taken from Distribution System Analysis Subcommittee - IEEE 34 Node Test Feeder (2017).

Annex 7

Spots load data

Node	Load Model	Ph-1 (kW)	Ph-1 (kvar)	Ph-2 (kW)	Ph-2 (kvar)	Ph-3 (kW)	Ph-3 (kvar)	Ph-4 (kvar)
860	Y-PQ	20	16	20	16	20	860	16
840	Y-I	9	7	9	7	9	840	7
844	Y-Z	135	105	135	105	135	844	105
848	D-PQ	20	16	20	16	20	848	16
890	D-I	150	75	150	75	150	890	75
830	D-Z	10	5	10	5	25	830	10

Note. Data taken from Distribution System Analysis Subcommittee - IEEE 34 Node Test Feeder (2017).

Annex 8

Distributed load data

Node A	Node B	Load Model	Ph-1 (kW)	Ph-1 (kvar)	Ph-2 (kW)	Ph-2 (kvar)	Ph-3 (kW)	Ph-3 (kvar)
802	806	Y-PQ	0	0	30	15	25	14
808	810	Y-I	0	0	16	8	0	0
818	820	Y-Z	34	17	0	0	0	0
820	822	Y-PQ	135	70	0	0	0	0
816	824	D-I	0	0	5	2	0	0
824	826	Y-I	0	0	40	20	0	0
824	828	Y-PQ	0	0	0	0	4	2
828	830	Y-PQ	7	3	0	0	0	0

854	856	Y-PQ	0	0	4	2	0	0
832	858	D-Z	7	3	2	1	6	3
858	864	Y-PQ	2	1	0	0	0	0
858	834	D-PQ	4	2	15	8	13	7
834	860	D-Z	16	8	20	10	110	55
860	836	D-PQ	30	15	10	6	42	22
836	840	D-I	18	9	22	11	0	0
862	838	Y-PQ	0	0	28	14	0	0
842	844	Y-PQ	9	5	0	0	0	0
844	846	Y-PQ	0	0	25	12	20	11
846	848	Y-PQ	0	0	23	11	0	0

Note. Data taken from Distribution System Analysis Subcommittee - IEEE 34 Node Test Feeder (2017).